

# Electromagnetic Properties of the $\Delta(1232)$

A. J. Buchmann<sup>1</sup>, E. Hernández<sup>2</sup>, and Amand Faessler<sup>1</sup>

<sup>1</sup> Institut für Theoretische Physik, Universität Tübingen  
Auf der Morgenstelle 14, D-72076 Tübingen, Germany

<sup>2</sup> Grupo de Física Nuclear, Universidad de Salamanca  
E-37008 Salamanca, Spain

June 30, 2021

## Abstract

We calculate the electromagnetic moments and radii of the  $\Delta(1232)$  in the nonrelativistic quark model, including two-body exchange currents. We show that two-body exchange currents lead to nonvanishing  $\Delta$  and  $N \rightarrow \Delta$  transition quadrupole moments even if the wave functions have no  $D$ -state admixture. The usual explanation based on the single-quark transition model involves  $D$ -state admixtures but no exchange currents. We derive a parameter-free relation between the  $N \rightarrow \Delta$  transition quadrupole moment and the neutron charge radius, namely  $Q_{N \rightarrow \Delta} = \frac{1}{\sqrt{2}} r_n^2$ . Furthermore, we calculate the  $M1$  and  $E2$  amplitudes for the process  $\gamma + N \rightarrow \Delta$ . We find that the  $E2$  amplitude receives sizeable contributions from exchange currents. These are more important than the ones which result from  $D$ -state admixtures due to tensor forces between quarks if a reasonable quark core radius of about 0.6 fm is used. We obtain a ratio of  $E2/M1 = -3.5\%$ .

## 1. Introduction

Low-energy electromagnetic properties of baryons, such as charge radii, magnetic moments and quadrupole moments, are very useful observables. In particular,  $\Delta$  electromagnetic properties provide valuable information on the quark-quark interaction that would otherwise be quite difficult to obtain. For example, while the nucleon wave function may contain a small D-state admixture and may therefore be deformed, angular momentum selection rules do not allow a spin 1/2 particle to have a nonzero quadrupole moment. However, as a spin 3/2 particle, the  $\Delta$  can have an observable quadrupole moment. If this could be measured, it would provide additional constraints on the magnitude of the D-state admixture in baryon ground-state wave functions.

In addition to the electromagnetic moments and radii of the  $\Delta$ , the electromagnetic  $\gamma + N \rightarrow \Delta$  transition form factors have received considerable attention during recent years. The reason is clear. While the magnetic and quadrupole moments of the  $\Delta$  are very hard to measure, there are new high-precision pionproduction experiments with real and virtual photons in the  $\Delta$ -resonance region [1] which will provide accurate data on the electric quadrupole ( $E2$ ) and magnetic dipole ( $M1$ ) parts of the amplitude. These transition multipoles are sensitive to details of the quark dynamics. In particular, the  $E2$  amplitude is crucial in getting a handle on the tensor forces between quarks and the related question of the deformation of the nucleon.

It has long been known that the reaction  $\gamma + p \rightarrow \Delta^+$  poses a problem for the additive quark model. The additive quark model predicts a relation between the  $M1$  transition moment and the proton magnetic moment [2]

$$\mu_{p \rightarrow \Delta^+} = \frac{2\sqrt{2}}{3} \mu_p. \quad (1)$$

Furthermore, it predicts that the  $p \rightarrow \Delta^+$  quadrupole transition moment is exactly zero [3]

$$Q_{p \rightarrow \Delta^+} = 0. \quad (2)$$

Both results contradict experimental findings. Eq.(1) gives  $\mu_{p \rightarrow \Delta^+} = 2.63 \mu_N$  if the experimental proton magnetic moment is used. This is about 30% lower than the empirical value  $3.5(2) \mu_N$ [4]. Also, the empirical quadrupole transition moment is small, but clearly nonzero [5]. Various corrections to the simple nonrelativistic quark model (NRQM) results have been considered. There are several works [6, 7, 8] which include  $D$ -state admixtures to the  $N$  and  $\Delta$  ground state resulting from one-gluon exchange induced tensor forces. The inclusion of these  $D$ -states leads to a nonvanishing  $E2$  transition amplitude; however, the effect of  $D$ -state admixtures on the  $M1$  amplitude slightly increases the discrepancy between theory and experiment. Other authors calculate relativistic corrections to the single-quark current [9, 10, 11]. These corrections, although they are significant, are too small to account for the data. The role of pions has been studied mainly in the framework of the bag model [12], in effective Lagrangian models [13, 14, 15, 16], or in the Skyrme model [17, 18].

Recently, Robson [19] calculated the  $A^{3/2}$  and  $A^{1/2}$  helicity amplitudes for the  $N \rightarrow \Delta$  transition including the pion pair exchange current but did not properly include the pionic current contribution. Also the  $E2$  contribution to the helicity amplitudes was omitted in this first calculation. The contribution of pion tensor forces to the  $E2$  transition was calculated in ref. [20], but in this work exchange current corrections were omitted. Most calculations of

electromagnetic properties in the constituent quark model (CQM) have been performed in the so-called impulse approximation, which assumes that the total electromagnetic current of the quarks is given by a sum of *free* quark currents. However, a calculation based on the impulse approximation is incomplete because it violates current conservation. Current conservation demands that the total electromagnetic current operator of bound quarks necessarily consist of two pieces: the one-body quark currents and the two-body exchange currents associated with the interactions responsible for quark binding.

In two previous papers [21, 22] we have investigated the effect of two-body exchange currents on the charge and magnetic form factors of the nucleon. We have shown that two-body gluon and pion exchange currents are essential in simultaneously describing proton and neutron charge radii and the positive parity excitation spectrum of the nucleon with a single set of parameters. In particular, by including gluon and pion exchange currents we were able to get a non-zero neutron charge radius of the right size. Using ground state wave functions we derived a relation between the neutron charge radius, the  $\Delta - N$  mass splitting, and the quark core radius  $b$ , namely  $r_n^2 = -b^2(M_\Delta - M_N)/M_N$ , which clearly shows the underlying connection between the excitation spectrum of the nucleon and its electromagnetic properties. Although this relation was derived with ground state wave functions, it remains approximately valid even after the inclusion of configuration mixing [21]. With respect to the magnetic moments, we have shown that exchange currents give individually large corrections but tend to cancel each other globally [22, 23], provided that the oscillator parameter is consistent with the one required to describe the experimental neutron charge radius. Finally, we have noted that although the direct effect of pions on electromagnetic properties was not particularly large, their inclusion was essential for a satisfactory description of the data.

In this work we extend our study of two-body exchange currents to the electromagnetic moments and radii of the  $\Delta$ . Furthermore, we calculate the magnetic and quadrupole  $N - \Delta$  transition moments and the corresponding helicity amplitudes  $A_{3/2}$  and  $A_{1/2}$  for the photoexcitation of the  $\Delta$ . Instead of focusing on just one observable (e.g.  $E2/M1$ ), we simultaneously calculate a number of important low-energy observables including the magnetic and quadrupole moments, and the charge and magnetic radii of *both* the nucleon and the  $\Delta$ , using a single set of parameters. In addition to the gluon, pion, and confinement exchange currents considered previously, we include the  $\sigma$ -exchange current as suggested by chiral symmetry. The aim of the present paper is to study the role of two-body exchange currents in  $\Delta$  electromagnetic properties. In order to isolate and emphasize their contribution and to keep calculations to a simple level we will take pure  $L = 0$ , ground state, harmonic oscillator, orbital wave functions for both the nucleon and  $\Delta$ .

We show that two-body currents yield substantial corrections for the quadrupole moment of the  $\Delta$  and the quadrupole transition moment. We find that the  $C2$ -amplitude is largely governed by the spin-dependent two-body pieces in the charge density operator, which in the long wave-length limit also determine the  $E2$ -amplitude in photo-pionproduction by application of Siegert's theorem. This implies that the  $E2$ -transition to the  $\Delta$  is presumably to a large extent a *two-quark spin-flip* transition.

The paper is organized as follows. In sect. 2, we review the chiral constituent quark model which includes not only gluon, but also pion and sigma-meson exchange between constituent quarks. Then, we list the two-body current operators connected with these quark-quark interactions (sect. 3). Various electromagnetic observables of the  $\Delta - N$  system are calculated and discussed in sect. 4. The main results of this work are summarized in sect. 5.

## 2. The Constituent Quark Model

It is nowadays understood that constituent quarks are quasi-particles, i.e. bare quarks surrounded by a polarization cloud of quark-antiquark pairs that are continuously excited from the QCD vacuum [24]. Constituent quarks are therefore complicated objects. They have a mass  $m_q \approx M_N/3$  and a finite hadronic size\*: The constituent quark mass generation is intimately related to the spontaneously broken chiral symmetry of QCD, i.e. to the fact that the QCD vacuum is not chirally invariant. The concept of a massive constituent quark incorporates much of the complexity of QCD in the low-energy domain of hadron physics. However, there are still some residual interactions between the constituent quarks. These simulate those dynamical features of QCD that are not yet included in the free quasi-particle description.

### 2.1. The Hamiltonian

We consider a baryon as a nonrelativistic three-quark system, which, in the case of equal quark masses  $m_q$ , is described by the Hamiltonian †

$$H = \sum_{i=1}^3 \left( m_q + \frac{\mathbf{p}_i^2}{2m_q} \right) - \frac{\mathbf{P}^2}{6m_q} + \sum_{i<j}^3 V^{conf}(\mathbf{r}_i, \mathbf{r}_j) + \sum_{i<j}^3 V^{res}(\mathbf{r}_i, \mathbf{r}_j), \quad (3)$$

where  $\mathbf{r}_i$ ,  $\mathbf{p}_i$  are the spatial and momentum coordinates of the  $i$ -th quark, respectively. The Hamiltonian of eq.(3) consists of the standard nonrelativistic kinetic energy, a confinement potential and residual interactions  $V^{res}$  (see fig.1) which model the relevant properties of QCD.

Asymptotic freedom is modelled in the CQM by the one-gluon exchange interaction,  $V^{OGEP}$ , of fig.1(a) which was first introduced by De Rujula, Glashow and Georgi in 1975 [26]:

$$\begin{aligned} V^{OGEP}(\mathbf{r}_i, \mathbf{r}_j) = & \frac{\alpha_s}{4} \boldsymbol{\lambda}_i \cdot \boldsymbol{\lambda}_j \left\{ \frac{1}{r} - \frac{\pi}{m_q^2} \left( 1 + \frac{2}{3} \boldsymbol{\sigma}_i \cdot \boldsymbol{\sigma}_j \right) \delta(\mathbf{r}) - \frac{1}{4m_q^2} \frac{1}{r^3} (3\boldsymbol{\sigma}_i \cdot \hat{\mathbf{r}} \boldsymbol{\sigma}_j \cdot \hat{\mathbf{r}} - \boldsymbol{\sigma}_i \cdot \boldsymbol{\sigma}_j) \right. \\ & - \frac{1}{2m_q^2} \frac{1}{r^3} \left[ 3 \left( \mathbf{r} \times \frac{1}{2} (\mathbf{p}_i - \mathbf{p}_j) \right) \cdot \frac{1}{2} (\boldsymbol{\sigma}_i + \boldsymbol{\sigma}_j) \right. \\ & \left. \left. - \left( \mathbf{r} \times \frac{1}{2} (\mathbf{p}_i + \mathbf{p}_j) \right) \cdot \frac{1}{2} (\boldsymbol{\sigma}_i - \boldsymbol{\sigma}_j) \right] \right\}, \quad (4) \end{aligned}$$

where  $\mathbf{r} = \mathbf{r}_i - \mathbf{r}_j$ ;  $\boldsymbol{\sigma}_i$  is the usual Pauli spin matrix, and  $\boldsymbol{\lambda}_i$  is the color operator of the  $i$ -th quark. The one-gluon exchange potential has the correct spin-color structure of QCD at short distances.

Chiral symmetry is probably the most important feature of QCD in the nonperturbative regime. Its importance for hadron physics has been highlighted in recent reviews [27]. The spontaneous breaking of chiral symmetry (SBCS) by the physical vacuum is responsible for the constituent quark mass generation and the appearance of pseudoscalar Goldstone bosons ( $\pi$ -mesons) together with their massive scalar partners ( $\sigma$ -mesons) which couple to the constituent quarks. In the chiral CQM [28], this is modelled in lowest order by

\*In this work we use  $r_q = 0.4$  fm (see eq.(9)).

†For recent reviews of the CQM see ref.[25].

introducing one-pion and one-sigma exchange potentials between constituent quarks (see fig.1(b-c)) [29, 30]:

$$V^{OPEP}(\mathbf{r}_i, \mathbf{r}_j) = \frac{g_{\pi q}^2}{4\pi(4m_q^2)} \frac{\Lambda^2}{\Lambda^2 - \mu^2} \boldsymbol{\tau}_i \cdot \boldsymbol{\tau}_j \boldsymbol{\sigma}_i \cdot \nabla_r \boldsymbol{\sigma}_j \cdot \nabla_r \left( \frac{e^{-\mu r}}{r} - \frac{e^{-\Lambda r}}{r} \right) \quad (5)$$

$$V^{OSEP}(\mathbf{r}_i, \mathbf{r}_j) = -\frac{g_{\sigma q}^2}{4\pi} \frac{\Lambda^2}{\Lambda^2 - m_\sigma^2} \left( \frac{e^{-m_\sigma r}}{r} - \frac{e^{-\Lambda r}}{r} \right) \quad (6)$$

where  $r = |\mathbf{r}| = |\mathbf{r}_i - \mathbf{r}_j|$  and  $\mu$  is the pion mass. Here,  $\boldsymbol{\tau}_i$  denotes the isospin of the  $i$ -th quark. The parameters of the  $\sigma$ -exchange potential  $V^{OSEP}$  are fixed by the ones of the  $\pi$ -exchange potential and the constituent quark mass [30] via the chiral symmetry constraints

$$\begin{aligned} \frac{g_{\sigma q}^2}{4\pi} &= \frac{g_{\pi q}^2}{4\pi} = \frac{f_{\pi q}^2}{4\pi} \left( \frac{2m_q}{\mu} \right)^2; \\ m_\sigma^2 &\approx (2m_q)^2 + \mu^2 \\ \Lambda_\pi &= \Lambda_\sigma = \Lambda \equiv \Lambda_{SBCS}. \end{aligned} \quad (7)$$

The terms in eq.(5) and eq.(6) involving the chiral cut-off  $\Lambda$  result from the use of  $\pi q$  and  $\sigma q$  vertex functions in momentum space of the form

$$F_{\pi q}(\mathbf{k}^2) = \left( \frac{\Lambda^2}{\Lambda^2 + \mathbf{k}^2} \right)^{1/2}, \quad (8)$$

where  $\mathbf{k}$  is the three-momentum of the pion. Thus, the chiral symmetry breaking scale  $\Lambda$  is related to the hadronic size of the constituent quark via the usual definition

$$r_{\pi q}^2 = -6 \frac{d}{d\mathbf{k}^2} F_{\pi q}(\mathbf{k}^2) |_{\mathbf{k}^2=0} = \frac{3}{\Lambda^2}. \quad (9)$$

This finite hadronic size of the constituent quarks is denoted by the extended vertices in fig.1. The larger  $\Lambda$ , the more point-like the constituent quark. For  $\Lambda \rightarrow \infty$  the one-pion exchange potential of eq.(5) is unregularized and we recover a  $\delta$ -function interaction between point-like constituent quarks. We usually take for the hadronic size of the constituent quarks  $r_q = 0.4$  fm, i.e.  $\Lambda = 4.2$  fm<sup>-1</sup> in connection with the vertex function of eq.(8).

It should be emphasized that we introduce  $\pi$ - and  $\sigma$ -mesons as fundamental fields (Goldstone bosons and their chiral partners) and not as  $q\bar{q}$  composites. One may also argue that the vertex function of eq.(8) describes *both* the hadronic size of the pion and of the constituent quarks.

Finally, in the CQM the confinement of quarks and gluons is modelled by a linear or quadratic two-body quark-quark potential. According to Shuryak [24], the confinement scale is related to the chiral symmetry breaking scale by  $\Lambda_{conf} \approx \Lambda_{SBCS}/3$ . This means that the distances where confinement effects become important are somewhat larger than the distances where chiral symmetry is broken. However, the boundary between the two mechanisms is not very well defined. Here, we employ a two-body harmonic oscillator confinement potential

$$V^{conf}(\mathbf{r}_i, \mathbf{r}_j) = -a_c \boldsymbol{\lambda}_i \cdot \boldsymbol{\lambda}_j (\mathbf{r}_i - \mathbf{r}_j)^2. \quad (10)$$

## 2.2. Baryon wave function and determination of parameters

The total baryon wave function  $\Phi_{N(\Delta)}$  is an inner product of the orbital, spin-isospin, and color wave function and given by

$$| \Phi_{N(\Delta)} \rangle = (1/\sqrt{3\pi b^2})^{3/2} \exp(-(\boldsymbol{\rho}^2/4b^2 + \boldsymbol{\lambda}^2/3b^2)) | ST \rangle^{N(\Delta)} \times | [111] \rangle_{color}^{N(\Delta)}, \quad (11)$$

where the Jacobi coordinates  $\boldsymbol{\rho}$  and  $\boldsymbol{\lambda}$  are defined as  $\boldsymbol{\rho} = \mathbf{r}_1 - \mathbf{r}_2$  and  $\boldsymbol{\lambda} = \mathbf{r}_3 - (\mathbf{r}_1 + \mathbf{r}_2)/2$ . With the Hamiltonian of eq.(3) and the wave function of eq.(11) it is straightforward to calculate the nucleon mass. One obtains

$$\begin{aligned} M_N(b) = & 3m_q + \frac{3}{2m_q b^2} + V^{conf}(b) - 2\alpha_s \sqrt{\frac{2}{\pi}} \frac{1}{b} + \frac{1}{3} \frac{\alpha_s}{m_q^2} \frac{1}{\sqrt{2\pi}} \frac{1}{b^3} \\ & - \frac{5}{4} \delta_\pi(b) + V^\sigma(b), \end{aligned} \quad (12)$$

$$\begin{aligned} M_\Delta(b) = & 3m_q + \frac{3}{2m_q b^2} + V^{conf}(b) - 2\alpha_s \sqrt{\frac{2}{\pi}} \frac{1}{b} + \frac{5}{3} \frac{\alpha_s}{m_q^2} \frac{1}{\sqrt{2\pi}} \frac{1}{b^3} \\ & - \frac{1}{4} \delta_\pi(b) + V^\sigma(b), \end{aligned} \quad (13)$$

where the individual terms in eqs.(12,13) are the nonrelativistic kinetic energy, quadratic confinement, gluon, pion, and sigma contributions, respectively. The confinement contribution to the nucleon and  $\Delta$  mass is given by

$$V^{conf}(b) = 24a_c b^2, \quad (14)$$

and the  $\sigma$ -meson potential contribution is

$$V^\sigma(b) = -6 \frac{\Lambda^2}{\Lambda^2 - m_\sigma^2} \frac{g_{\sigma q}^2}{4\pi} \frac{1}{\sqrt{2\pi}} \frac{1}{b} \left\{ \left( 1 - \sqrt{\pi} \left( \frac{m_\sigma b}{\sqrt{2}} \right) e^{m_\sigma^2 b^2 / 2} \operatorname{erfc} \left( \frac{m_\sigma b}{\sqrt{2}} \right) \right) - (m_\sigma \leftrightarrow \Lambda) \right\}. \quad (15)$$

Explicit expressions for  $\delta_g$ ,  $\delta_\pi$  are given below. Subtracting eq.(12) from eq.(13) all spin-independent terms drop out and one gets

$$M_\Delta - M_N = \delta_g(b) + \delta_\pi(b), \quad (16)$$

where  $\delta_\pi(b)$  and  $\delta_g(b)$  are the *spin-dependent* pion and gluon contributions to the  $\Delta - N$  mass splitting.

The parameters of the model are: (i) the harmonic oscillator parameter  $b$ , (ii) the confinement strength  $a_c$ , (iii) the strong coupling constant  $\alpha_s$ , (iv) the cut-off mass  $\Lambda$  in the pion-quark and sigma-quark interaction. For the constituent quark mass we choose  $m_q = M_N/3 = 313$  MeV. The parameters  $a_c$ ,  $\alpha_s$ , and  $b$  are determined from the three conditions

$$M_N(b) = 3m_q = 939 \text{ MeV}, \quad M_\Delta - M_N = \delta_\pi(b) + \delta_g(b) = 293 \text{ MeV}, \quad \frac{\partial M_N(b)}{\partial b} = 0, \quad (17)$$

as previously described [21]. The gluon ( $\delta_g$ ) and pion ( $\delta_\pi$ ) contributions to the  $\Delta - N$  mass splitting are calculated as

$$\delta_g(b) = \frac{4\alpha_s}{3\sqrt{2\pi} m_q^2 b^3}, \quad (18)$$

$$\delta_\pi(b) = -4 \frac{\Lambda^2}{\Lambda^2 - \mu^2} \frac{f_{\pi q}^2}{4\pi\mu^2} \sqrt{\frac{2}{\pi}} \frac{1}{b} \left\{ \mu^2 \left( 1 - \sqrt{\pi} \left( \frac{\mu b}{\sqrt{2}} \right) e^{\mu^2 b^2/2} \operatorname{erfc} \left( \frac{\mu b}{\sqrt{2}} \right) \right) - (\mu \leftrightarrow \Lambda) \right\}, \quad (19)$$

respectively. In the following we write  $\delta_\pi(b) = \delta_{\pi_\mu}(b) - \delta_{\pi_\Lambda}(b)$  for brevity. Numerical values for the individual contributions to the nucleon mass and to the  $\Delta - N$  mass splitting are listed in table 2.

The residual interactions will admix higher excited states to the pure  $(0s)^3$  ground state wave functions of eq.(11) (configuration mixing). If we restrict ourselves to  $2\hbar\omega$  excitations, we have four excited states ( $\Phi_{S'_S}^N, \Phi_{S_M}^N, \Phi_{D_M}^N, \Phi_{P_A}^N$ ) for the  $N$  and three excited states ( $\Phi_{D_S}^\Delta, \Phi_{D_M}^\Delta$ ) for the  $\Delta$ . The subscripts  $L_{sym}$  describe the orbital angular momentum ( $L$ ) and the symmetry ( $sym$ ) of the orbital wave function under particle exchange. Here,  $S$  denotes symmetric,  $M$  mixed symmetric and  $A$  antisymmetric orbital wave functions. The  $N$  and  $\Delta$  wave functions are then given by

$$\begin{aligned} \Phi_N &= a_{S_S} \Phi_{S'_S}^N + a_{S'_S} \Phi_{S'_S}^N + a_{S_M} \Phi_{S_M}^N + a_{D_M} \Phi_{D_M}^N + a_{P_A} \Phi_{P_A}^N \\ \Phi_\Delta &= b_{S_S} \Phi_{S'_S}^\Delta + b_{S'_S} \Phi_{S'_S}^\Delta + b_{D_S} \Phi_{D_S}^\Delta + b_{D_M} \Phi_{D_M}^\Delta. \end{aligned} \quad (20)$$

A detailed description of these wave functions can be found in ref.[37].

In ref.[21, 22] we used the wave functions of eq.(20) and simultaneously calculated the positive parity excitation spectrum of the  $N$  and  $\Delta$  and the electromagnetic properties of the nucleon. In most cases this slightly improved the results for the electromagnetic properties in comparison to a pure ground state calculation. The main effect of configuration mixing was to increase the pion contribution and to reduce the gluon contribution to various observables. In addition, the value of the harmonic oscillator constant  $b$  was slightly reduced with respect to a pure  $L = 0$  ground state calculation.

In this work, we use the ground state wave function of eq.(11) since this considerably simplifies calculations. Because the mixing amplitudes, as obtained by different groups [6, 8, 9, 10, 21] are small, our calculation provides the dominant part of the exchange current contribution to different observables. Certainly, the simple relations between different low energy observables, which we will derive in sect. 4 do not hold exactly in a more complete calculation with configuration mixed wave functions. Still, we expect them to hold in good approximation, for example,  $r_n^2 = -b^2(M_\Delta - M_N)/M_N$  holds true at the level of 23% or better even if configuration mixed wave functions are used [21]. Therefore, we think that our conclusions concerning the role of exchange currents will remain true also in a more consistent calculation employing the full wave functions of eq.(20). We will discuss this in more detail in sect. 4.

### 3. Electromagnetic currents

The interaction of the external electromagnetic field  $A^\mu(x) = (\Phi(x), \mathbf{A}(x))$  with a hadronic system is described by the Hamilton operator

$$H_{em} = \int d^4x J_\mu(x) A^\mu(x). \quad (21)$$

where  $J_\mu(x) = (\rho(x), -\mathbf{J}(x))$  is the four-vector current density of the quarks inside the system. Thus, in a quark model description we must know the charge and current operators of the interacting quarks in order to describe the electromagnetic properties of the baryon.

### 3.1. One-body current

First, we consider the standard nonrelativistic one-body charge and current operators of point-like constituent quarks (see fig.2a)

$$\begin{aligned}\rho_{imp}^{IS/IV}(\mathbf{r}_i, \mathbf{q}) &= e_i e^{i\mathbf{q}\cdot\mathbf{r}_i} \\ \mathbf{J}_{imp}^{IS/IV}(\mathbf{r}_i, \mathbf{q}) &= \frac{e_i}{2m_q} \left( i [\boldsymbol{\sigma}_i \times \mathbf{p}_i, e^{i\mathbf{q}\cdot\mathbf{r}_i}] + \{ \mathbf{p}_i, e^{i\mathbf{q}\cdot\mathbf{r}_i} \} \right),\end{aligned}\quad (22)$$

where  $e_i = \frac{1}{6}e(1 + 3\boldsymbol{\tau}_{i3})$  is the quark charge operator and  $\mathbf{q}$  is the three-momentum transfer of the photon. Here and in the following  $\boldsymbol{\tau}_{i3}$  denotes the third component of the isospin of the  $i$ -th quark. The decomposition of eq.(22) into isoscalar (IS) or isovector (IV) currents is obtained by taking only the first or second term of the quark charge operator into account. Note that we do not use any anomalous magnetic moments for the constituent quarks [31].

### 3.2. Two-body exchange currents

In most applications of the CQM the total electromagnetic current has been approximated by a sum of single-quark currents of the form of eq.(22)

$$J_{total}^\mu \approx \sum_{i=1}^3 J_{imp}^\mu(i). \quad (23)$$

However, the current of eq.(23) is not conserved in the presence of various residual interactions between the quarks. In a bound system of quarks the electromagnetic current operator is not simply a sum of free quark currents as in eq.(23) but necessarily contains various two-body currents for the total electromagnetic current to be conserved. The spatial parts of these two-body currents are closely related to the quark-quark potentials from which they can be derived by minimal substitution [22].

In the following, we list the two-body charge and current operators employed in this work. They have been derived by a nonrelativistic expansion of the Feynman diagrams of fig.2(b-e) up to lowest nonvanishing order. Only, in the case of the isovector pion pair-current we also list the next-to-leading order term for reasons discussed in sect. 4.3. For the gluon and pion exchange currents we obtain [21, 22]

$$\begin{aligned}\rho_{gq\bar{q}}^{IS/IV}(\mathbf{r}_i, \mathbf{r}_j, \mathbf{q}) &= -i \frac{\alpha_s}{16m_q^3} \boldsymbol{\lambda}_i \cdot \boldsymbol{\lambda}_j \left\{ e_i e^{i\mathbf{q}\cdot\mathbf{r}_i} [\mathbf{q} \cdot \mathbf{r} + (\boldsymbol{\sigma}_i \times \mathbf{q}) \cdot (\boldsymbol{\sigma}_j \times \mathbf{r})] + (i \leftrightarrow j) \right\} \frac{1}{r^3}, \\ \mathbf{J}_{gq\bar{q}}^{IS/IV}(\mathbf{r}_i, \mathbf{r}_j, \mathbf{q}) &= -\frac{\alpha_s}{4m_q^2} \boldsymbol{\lambda}_i \cdot \boldsymbol{\lambda}_j \left\{ e_i e^{i\mathbf{q}\cdot\mathbf{r}_i} \frac{1}{2} (\boldsymbol{\sigma}_i + \boldsymbol{\sigma}_j) \times \mathbf{r} + (i \leftrightarrow j) \right\} \frac{1}{r^3};\end{aligned}\quad (24)$$

$$\begin{aligned}\rho_{\pi q\bar{q}}^{IS}(\mathbf{r}_i, \mathbf{r}_j, \mathbf{q}) &= \frac{ie}{6} \frac{g_{\pi q}^2}{4\pi(4m_q^3)} \frac{\Lambda^2}{\Lambda^2 - \mu^2} \boldsymbol{\tau}_i \cdot \boldsymbol{\tau}_j \left\{ e^{i\mathbf{q}\cdot\mathbf{r}_i} \boldsymbol{\sigma}_i \cdot \mathbf{q} \boldsymbol{\sigma}_j \cdot \nabla_{\mathbf{r}} + (i \leftrightarrow j) \right\} \left( \frac{e^{-\mu r}}{r} - \frac{e^{-\Lambda r}}{r} \right), \\ \mathbf{J}_{\pi q\bar{q}}^{IS}(\mathbf{r}_i, \mathbf{r}_j, \mathbf{q}) &= \frac{ie}{6} \frac{g_{\pi q}^2}{4\pi(8m_q^4)} \frac{\Lambda^2}{\Lambda^2 - \mu^2} \boldsymbol{\tau}_i \cdot \boldsymbol{\tau}_j \left\{ e^{i\mathbf{q}\cdot\mathbf{r}_i} \mathbf{q} \times \nabla_{\mathbf{r}} \boldsymbol{\sigma}_j \cdot \nabla_{\mathbf{r}} + (i \leftrightarrow j) \right\} \left( \frac{e^{-\mu r}}{r} - \frac{e^{-\Lambda r}}{r} \right).\end{aligned}\quad (25)$$

$$\rho_{\pi q\bar{q}}^{IV}(\mathbf{r}_i, \mathbf{r}_j, \mathbf{q}) = \frac{ie}{2} \frac{g_{\pi q}^2}{4\pi(4m_q^3)} \frac{\Lambda^2}{\Lambda^2 - \mu^2} \left\{ \boldsymbol{\tau}_{j3} e^{i\mathbf{q}\cdot\mathbf{r}_i} \boldsymbol{\sigma}_i \cdot \mathbf{q} \boldsymbol{\sigma}_j \cdot \nabla_{\mathbf{r}} + (i \leftrightarrow j) \right\} \left( \frac{e^{-\mu r}}{r} - \frac{e^{-\Lambda r}}{r} \right),$$



$$\begin{aligned}
\mathbf{J}_\pi^{IV}(\mathbf{r}_i, \mathbf{r}_j, \mathbf{q}) &= e \frac{g_{\pi q}^2}{4\pi(2m_q)^2} \frac{\Lambda^2}{\Lambda^2 - \mu^2} \left[ \left\{ (\boldsymbol{\tau}_i \times \boldsymbol{\tau}_j)_3 e^{i\mathbf{q}\cdot\mathbf{r}_i} \boldsymbol{\sigma}_i \boldsymbol{\sigma}_j \cdot \nabla_{\mathbf{r}} + (i \leftrightarrow j) \right\} \left( \frac{e^{-\mu r}}{r} - \frac{e^{-\Lambda r}}{r} \right) \right. \\
&+ \frac{i}{4m_q^2} \left\{ \boldsymbol{\tau}_{j3} e^{i\mathbf{q}\cdot\mathbf{r}_i} \mathbf{q} \times \nabla_{\mathbf{r}} \boldsymbol{\sigma}_j \cdot \nabla_{\mathbf{r}} + (i \leftrightarrow j) \right\} \left( \frac{e^{-\mu r}}{r} - \frac{e^{-\Lambda r}}{r} \right) \\
&\left. + (\boldsymbol{\tau}_i \times \boldsymbol{\tau}_j)_3 \boldsymbol{\sigma}_i \cdot \nabla_i \boldsymbol{\sigma}_j \cdot \nabla_j \int_{-1/2}^{1/2} dv e^{i\mathbf{q}\cdot(\mathbf{R}-rv)} \left( \mathbf{z}_\mu \frac{e^{-L_\mu r}}{L_\mu r} - \mathbf{z}_\Lambda \frac{e^{-L_\Lambda r}}{L_\Lambda r} \right) \right]. \quad (26)
\end{aligned}$$

The first two terms in eq.(26) are the leading order pion pair-current proportional to  $(\boldsymbol{\tau}_i \times \boldsymbol{\tau}_j)_3$  and its next-to-leading order relativistic correction proportional to  $\boldsymbol{\tau}_{j3}$  shown in fig. 2b. The third term in eq.(26) is the pionic current  $\mathbf{J}_{\gamma\pi\pi}^{IV}$  of fig. 2c. We have used the following abbreviations  $\mathbf{R} = (\mathbf{r}_i + \mathbf{r}_j)/2$ ,  $\mathbf{z}_m(\mathbf{q}, \mathbf{r}) = L_m \mathbf{r} + ivr\mathbf{q}$ , and  $L_m(q, v) = [\frac{1}{4}q^2(1-4v^2) + m^2]^{1/2}$ .

The scalar pair-current corresponding to a Lorentz-scalar interaction was previously [22] derived as:

$$\begin{aligned}
\rho_{scalar}^{IS/IV}(\mathbf{r}_i, \mathbf{r}_j, \mathbf{q}) &= \frac{1}{(2m_q)^3} \left\{ e^{i\mathbf{q}\cdot\mathbf{r}_i} e_i \left( \frac{3}{2}\mathbf{q}^2 - i\mathbf{q} \cdot \nabla_r + \frac{1}{2}\nabla_r^2 \right) V^{scalar}(\mathbf{r}_i, \mathbf{r}_j) + (i \leftrightarrow j) \right\} \\
\mathbf{J}_{scalar}^{IS/IV}(\mathbf{r}_i, \mathbf{r}_j, \mathbf{q}) &= -\frac{1}{2m_q^2} \left\{ e_i e^{i\mathbf{q}\cdot\mathbf{r}_i} \boldsymbol{\sigma}_i \times \mathbf{q} V^{scalar}(\mathbf{r}_i, \mathbf{r}_j) + (i \leftrightarrow j) \right\}. \quad (27)
\end{aligned}$$

Eq.(27) is used to calculate both the confinement- and  $\sigma$ -meson-exchange currents. To obtain the spatial part of this current directly from the potential one must reduce the relativistic scalar potential to the same order in  $1/m_q^2$  as the one-gluon exchange potential. By minimal substitution  $\mathbf{p}_i \rightarrow \mathbf{p}_i - e\mathbf{A}(\mathbf{r}_i)$  in the scalar potential and by adding the contribution of the commutator of the  $\mathcal{O}(1/m_q^2)$  term in the one-body charge density with the leading order scalar potential one obtains the scalar pair-current shown in fig.2e. This is explained in greater detail in ref. [22].

The total charge operator consists of the usual one-body charge operator and two-body charge operators due to the interaction between the quarks

$$\rho_{total}(\mathbf{q}) = \sum_{i=1}^3 \rho_{imp}(\mathbf{r}_i) + \sum_{i<j}^3 \left( \rho_{gq\bar{q}}(\mathbf{r}_i, \mathbf{r}_j) + \rho_{\pi q\bar{q}}(\mathbf{r}_i, \mathbf{r}_j) + \rho_{\sigma q\bar{q}}(\mathbf{r}_i, \mathbf{r}_j) + \rho_{conf}(\mathbf{r}_i, \mathbf{r}_j) \right). \quad (28)$$

Likewise the total current operator consists of the usual one-body operator and two-body exchange current operators tightly related to the different quark-quark interactions

$$\mathbf{J}_{total}(\mathbf{q}) = \sum_{i=1}^3 \mathbf{J}_{imp}(\mathbf{r}_i) + \sum_{i<j}^3 \left( \mathbf{J}_{gq\bar{q}}(\mathbf{r}_i, \mathbf{r}_j) + \mathbf{J}_\pi^{IV}(\mathbf{r}_i, \mathbf{r}_j) + \mathbf{J}_{\pi q\bar{q}}^{IS}(\mathbf{r}_i, \mathbf{r}_j) + \mathbf{J}_{\sigma q\bar{q}}(\mathbf{r}_i, \mathbf{r}_j) + \mathbf{J}_{conf}(\mathbf{r}_i, \mathbf{r}_j) \right). \quad (29)$$

The extent to which the spatial current satisfies the continuity equation with the potential used in sect. 2 has been discussed previously [22].

### 3.3. Electromagnetic size of the constituent quarks

In sect. 2 we have seen that constituent quarks have a finite hadronic size which is given by the hadronic form factor of eq.(8). Similarly, the *electromagnetic* size of the constituent quarks is described by a monopole form factor

$$F_{\gamma q}(\mathbf{q}^2) = \frac{1}{1 + \frac{1}{6}\mathbf{q}^2 r_{\gamma q}^2}. \quad (30)$$

In order to take the internal electromagnetic structure of the constituent quarks into account, the charge and current operators of the previous section must be multiplied by the form factor of eq.(30).

The finite electromagnetic radius  $r_{\gamma q}$  takes into account that constituent quarks are dressed particles, i.e. current quarks surrounded by a cloud of  $q\bar{q}$ -pairs. The dominant contributions come from quark-antiquark pairs with pion quantum numbers. Vector meson dominance relates the electromagnetic radius of the constituent quarks to the  $\rho$ -meson pole according to fig.3. The notion of a finite electromagnetic size of the constituent quarks has been used before [32, 33, 34]. While the mass and size of the constituent quarks are appreciably renormalized from the point particle values explicit calculation in the Nambu-Jona-Lasinio model shows that the anomalous magnetic moment of constituent quarks is small [34]. This was previously anticipated on general grounds [31].

#### 4. $\Delta$ electromagnetic properties

A hadron with spin  $J$  has, in general,  $2J + 1$  elastic electromagnetic form factors. This result can be deduced by writing the most general Lorentz-invariant expression for the electromagnetic current operator of a hadron with total angular momentum  $J$ . One then demands hermiticity, and that the diagonal matrix elements be invariant under time and parity transformations and satisfy the continuity equation for the electromagnetic current. This reduces the number of allowed form factors to  $2J + 1$ . The  $\Delta$  thus has four elastic form factors [35] (and references therein): the charge monopole  $F_{C0}$ , the charge quadrupole  $F_{C2}$ , the magnetic dipole  $F_{M1}$ , and the magnetic octupole  $F_{M3}$ . It turns out that the  $M3$  form factor vanishes exactly for the ground state wave functions considered in this work. In order to describe the electromagnetic  $N \rightarrow \Delta$  transition [36] one needs the transverse magnetic dipole  $F_{M1}^{N \rightarrow \Delta}$ , the transverse electric quadrupole  $F_{E2}^{N \rightarrow \Delta}$  and the charge quadrupole (longitudinal)  $F_{C2}^{N \rightarrow \Delta}$  transition form factors.

In this work we concentrate on electromagnetic moments and radii of the  $\Delta$ , where the nonrelativistic quark model is expected to work best. Unlike the full form factors, the results for these static properties can be obtained in terms of analytic expressions, which makes the relation between the electromagnetic properties of the nucleon and  $\Delta$  more transparent. In particular, the important role of non-valence quark degrees of freedom in various electromagnetic properties will become evident. A review of  $\Delta$  electromagnetic properties in the quark model has been given by Giannini [37].

##### 4.1. Charge Radii

Charge radii measure the spatial extension of the charge distribution inside the baryon. They contain information about non-valence quark degrees of freedom and about the finite electromagnetic size of the valence quarks. Quite generally, the charge radius is defined as the slope of the charge form factor at zero-momentum transfer

$$r_C^2 = -\frac{6}{F_C(0)} \frac{d}{d\mathbf{q}^2} F_C(\mathbf{q}^2) \Big|_{\mathbf{q}^2=0}, \quad (31)$$

where, according to the general definition of the elastic form factors [38],

$$F_C(\mathbf{q}^2) = \sqrt{4\pi} \langle JM_J=J \ TM_T \mid \frac{1}{4\pi} \int d\Omega_q \rho(\mathbf{q}) Y_0^0(\hat{\mathbf{q}}) \mid JM_J=J \ TM_T \rangle. \quad (32)$$

#### 4.1.1. Charge Radius of the $\Delta$

Using eq.(28) and the ground state wave functions of eq.(11), we obtain the following analytic expressions

$$r_{\Delta}^2 = b^2 + r_{\gamma q}^2 + \frac{b^2}{6m_q}(5\delta_g - \delta_{\pi}) + \frac{5}{6m_q^3}V^{conf} + r_{\sigma}^2. \quad (33)$$

Eq.(33) is valid for charged  $\Delta$  states, while  $r_{\Delta^0}^2$  is zero in the present model. The first two terms in eq.(33) are due to the one-body quark current including the finite electromagnetic size of the quarks, while the remaining terms represent the gluon, pion, confinement, and sigma exchange current contributions. An analytic expression for  $r_{\sigma}^2$  can be obtained by replacing  $V^{conf}$  by  $V^{\sigma}$  in eq.(4.11) of ref. [22]. Note that the spin-independent scalar two-body charge densities have the same isospin structure as the one-body charge density. Therefore, as in the case of the one-body charge density contribution, the spin-independent scalar exchange current contributions to the charge radii are identical for  $N$  and  $\Delta$ . Our numerical results are listed in table 3.

If we compare this with the corresponding result for the proton

$$r_p^2 = b^2 + r_{\gamma q}^2 + \frac{b^2}{2m_q}(\delta_g - \delta_{\pi}) + \frac{5}{6m_q^3}V^{conf} + r_{\sigma}^2 \quad (34)$$

and neutron

$$r_n^2 = -\frac{b^2}{3m_q}(\delta_g + \delta_{\pi}) = -b^2 \frac{M_{\Delta} - M_N}{M_N}, \quad (35)$$

we obtain from eqs.(33,34, 35) the parameter-independent result

$$r_{\Delta}^2 = r_p^2 - r_n^2. \quad (36)$$

Hence, the charge radius of the  $\Delta$  is equal to the isovector charge radius of the nucleon. Stated differently, the charge radius of the  $\Delta$  is somewhat larger than that of the proton, and the difference is given by the neutron charge radius. This is in agreement with other models of nucleon structure [39].

We have noted that the charge radius of the  $\Delta^0$  is exactly zero in this model. This is so, because all terms in eq.(28) yield contributions to the  $\Delta$  charge form factor which are proportional to the  $\Delta$  charge

$$e_{\Delta} = \frac{1}{2}(1 + 2M_T), \quad (37)$$

where  $M_T$  is the third component of the isospin of the  $\Delta$ . Therefore, the form factor of eq.(32) vanishes identically and the corresponding charge radius is zero.

In contrast to this, the neutron charge radius of eq.(35) is clearly nonzero, but in this case we also obtain a particularly simple result. Because the neutron charge radius is given by the difference of isoscalar and isovector radii, the contributions of the one-body charge density, the finite size of the quarks, and the spin-independent scalar (confinement and sigma) exchange currents all cancel in  $r_n^2$ . Only the spin-dependent pion and gluon exchange currents contribute to  $r_n^2$ . The gluon and pion exchange currents can be expressed in terms of  $\delta_{\pi}$  and  $\delta_g$ , i.e. the pion and gluon contribution to the  $N - \Delta$  mass splitting, because the exchange current operators have a structure similar to the corresponding potentials. The particular combination of  $\delta_{\pi}$  and  $\delta_g$  appearing in eq.(35) makes it possible to express  $r_n^2$

via the experimental  $\Delta - N$  mass splitting of eq.(17). Eq.(35) clearly shows that there is an intimate relation between: (i) the neutron charge radius, (ii) the spatial extension of the quark distribution inside the nucleon (the quark core radius  $b$ ), and (iii) the excitation energy to the first excited state of the nucleon. From eq.(35) we determine the quark core size as  $b = 0.612$  fm, if the experimental numbers for  $M_N$ ,  $M_\Delta$ , and  $r_n^2$  are substituted.

#### 4.1.2. Configuration mixing vs. exchange currents

Let us try to give a physical interpretation of the results of eq.(33,35). In previous works, the nonvanishing charge radius of the neutron was attributed to the perturbing effect of the color-magnetic interaction on the ground state wave function [40, 41]. The color-magnetic interaction provides a repulsive force between any two quarks which are in a symmetric spin state ( $S = 1$ ). This makes the  $\Delta$ -isobar heavier than the nucleon, since the former contains more spin symmetric quark pairs. Similarly, the color-magnetic force repels the two down quarks in the neutron which are necessarily in an  $S = 1$  state (Pauli principle). This leads to a negative tail in the neutron charge distribution and to a negative neutron charge radius. On the other hand, the  $\Delta^0$  is symmetric in spin space and the spin-dependent forces do not introduce any asymmetry between  $ud$  and  $dd$  quark pairs. Therefore, the charge radius of the  $\Delta^0$  is zero. Thus, the same physical mechanisms (one gluon- and one-pion exchange) are responsible for the  $\Delta - N$  mass splitting and the negative charge radius of the neutron.

We point out that this effect, which is usually described by a small admixture of the excited  $\Phi_{S_M}$  state of eq.(20) into the nucleon ground state wave function, *is much too small*. It is around  $r_n^2(imp) = -0.03$  fm<sup>2</sup> if a realistic quark core radius ( $b \approx 0.6$  fm) is used (see the discussion below fig.2 in ref. [21]). The success of previous impulse calculations for the neutron charge is bought by tolerating a severe inconsistency: a value of  $b \approx 0.5 - 0.6$  fm is typically used in the calculation of the excitation spectrum [7] while a value  $b \approx 1$  fm is employed in the neutron charge radius calculation [37]. In addition, a large quark core radius  $b \approx 1$  fm contradicts information from several other sources and seems to be ruled out [37].

The present explanation of the negative neutron charge radius is based on the spin-dependent two-body gluon- and pion *exchange current operators*. This allows to get the correct size of the neutron charge radius for a reasonably small quark core radius  $b \approx 0.6$  fm. The exchange currents which we discuss here are closely related to the spin-dependent terms in the potential which give rise to the  $\Phi_{S_M}$  state. Yet, there is an important difference between these two mechanisms. We will explain this in more detail in the next section.

Of course, in a fully consistent calculation both configuration mixing and exchange currents must be included and the question concerning their relative importance arises. In addition, the simple relation between the neutron charge radius and the  $N - \Delta$  mass splitting will be modified in a more consistent calculation. However, according to ref.[21] eq.(35) is satisfied to within 23% in a model with gluons only; in the model with gluons and pions it holds to within 12% even if configuration mixing is included. Therefore, we believe that eq.(35) correctly describes the physics behind the nonvanishing neutron charge radius and certain other observables, that are very sensitive to nonvalence quark degrees of freedom (gluons, pions, and sea-quarks).

In our previous calculation of the neutron charge form factor [21] including both configuration mixing and exchange currents we have seen that the neutron charge radius is clearly dominated by the gluon and pion quark-pair currents (see fig.2b-c) if a reasonably small quark core radius ( $b = 0.5 - 0.6$  fm) is used. This finding gets support from other sources.

For example, Christov *et al.* [44] find in their chiral Nambu-Jona-Lasinio type quark model that the neutron charge radius is completely dominated by sea-quarks and not by valence quark degrees of freedom. In the language of quark potential models, it is most natural to include these nonvalence quark degrees of freedom in electromagnetic observables in the form of *gluon and pion exchange currents*.

## 4.2. Quadrupole moments

QCD predicts effective tensor forces between quarks. Consequently, baryons should be deformed. Experiments at all major electron laboratories are being devoted to measuring this deformation by photo/electro-excitation of the  $\Delta$ -resonance [1]. From these measurements one hopes to extract the  $D$ -state probabilities  $a_D^2$  and  $b_D^2$  in eq.(20) and from these further information about the tensor force between quarks.

On the other hand, it is well known from nuclear physics that rigorous bounds on  $D$ -state admixtures are difficult to obtain from observables such as quadrupole and magnetic moments. For example, in the case of the deuteron, meson exchange current corrections destroy the direct relation between the  $D$ -state admixture and the measured magnetic and quadrupole moments. Before we can extract information about interquark forces from these observables, we must have some knowledge of the effect of exchange currents.

The quadrupole moment is defined as the  $q \rightarrow 0$  limit of the quadrupole form factor [38]

$$F_Q(\mathbf{q}^2) = -\frac{12\sqrt{5}\pi}{q^2} \langle JM_J=J TM_T | \frac{1}{4\pi} \int d\Omega_q \rho(\mathbf{q}) Y_0^2(\hat{\mathbf{q}}) | JM_J=J TM_T \rangle, \quad (38)$$

where  $J = T = 3/2$ .

### 4.2.1. Quadrupole moment of the $\Delta$

With the two-body charge densities employed in this work we derive a parameter-independent relation between the neutron charge radius and the quadrupole moment of the  $\Delta$

$$Q_\Delta = -b^2 \frac{(\delta_g + \delta_\pi)}{3m_q} e_\Delta = -b^2 \left( \frac{M_\Delta - M_N}{M_N} \right) e_\Delta = r_n^2 e_\Delta, \quad (39)$$

where  $e_\Delta = (1 + 2M_T)/2$  is the charge of the  $\Delta$ . Hence, for the  $\Delta^{++}$  we predict a quadrupole moment of  $Q_{\Delta^{++}} = -0.235 \text{ fm}^2$ . Numerical values for the other quadrupole moments are listed in table 4. A similar relation between the neutron charge radius and the  $\Delta$  quadrupole moment has been obtained on the basis of configuration mixing and a  $Q_{\Delta^{++}} = -0.093 \text{ fm}^2$  has been found [45]. We will discuss the relation between exchange current and configuration mixing (tensor force) contributions to  $Q_\Delta$  in more detail below.

The first thing one notices is that even without an explicit  $D$ -state admixture in the  $\Delta$  wave function, we have obtained a nonvanishing quadrupole moment. In the following, we provide an explanation for this result. According to the definition of the quadrupole form factor of eq.(38), the charge density operator must contain a term  $Y^{[2]}(\hat{\mathbf{q}})$ , otherwise the quadrupole form factor vanishes, due to the orthogonality of the spherical harmonics. For example, after expanding the plane wave in eq.(22), the one-body charge operator is proportional to

$$\rho_{[1]}^{imp} \propto \left[ Y^{[l]}(\hat{\boldsymbol{\rho}}) \times Y^{[l]}(\hat{\mathbf{q}}) \right]^{[0]}. \quad (40)$$

For a pure  $S$ -state  $\Delta$  wave function only the term  $l = 0$  can contribute and consequently a  $Y^{[2]}(\hat{\mathbf{q}})$  term is not allowed. On the other hand, the two-body gluon and pion charge

densities contain a rank 2 tensor in spin space

$$\rho_{[2]}^{exc} \propto \left[ [\boldsymbol{\sigma}_i^{[1]} \times \boldsymbol{\sigma}_j^{[1]}]^{[2]} \times [Y^{[l]}(\hat{\boldsymbol{\rho}}) \times Y^{[2]}(\hat{\mathbf{q}})]^{[2]} \right]^{[0]}. \quad (41)$$

Therefore, it is possible to have a  $Y^{[2]}(\hat{\mathbf{q}})$  part even if  $l = 0$  and the quarks are all in S-states. That is why the two-body charge densities derived from fig.2b and fig.2d lead to a nonvanishing quadrupole moment. To state this in more physical terms we can say that due to the spin-dependent interaction currents between the quarks, the system can absorb a  $C2$  or  $E2$  photon.

As is evident from eqs.(39), these two-body charge densities describe the same gluon and pion degrees of freedom which are responsible for the tensor forces between quarks. The physical interpretation of both types of contributions (tensor force vs. two-body current) to the quadrupole moment is, however, quite different. This is illustrated in fig.4(a-b). The *two-body* gluon and pion pair-charge densities of fig.4b describe, as their name implies, the excitation of quark-antiquark pairs by the photon, or, stated differently, the absorption of a  $C2$  photon on *two quarks*. On the other hand, in fig.4a the photon is absorbed by a *single quark*, which remains in a positive energy state between the absorption of the photon and the emission of the gluon or pion. There is no electromagnetic coupling of the photon to the quark-antiquark pairs inside the  $\Delta$  in this case. In fig.4a, gluon and pion degrees of freedom show up as tensor force induced  $D$ -state admixtures to ground state wave functions (see eq.(20)). In most applications of the CQM, the single-quark current of fig.4a has been used to estimate the effect of the one-gluon exchange potential on electromagnetic properties. Our results show that this is not a good approximation for the charge properties of the  $\Delta$ , which are appreciably affected by exchange currents. This is opposite to what one finds in light nuclei. For example, the deuteron quadrupole moment is mainly caused by the  $D$ -wave in the deuteron and exchange currents, for example, the pion-pair charge density in eq.(25), provide only a correction of about 4% [42].

Obviously, a complete calculation comprises both  $D$ -waves in the nucleon and the exchange currents discussed in this work. Corrections due to  $D$ -waves will modify the simple result of eq.(39). However, according to our previous experience with the neutron charge radius, we expect it to remain largely valid. Let us discuss this more quantitatively. Including configuration mixing but no exchange currents one obtains neglecting the small  $b_D^2$  contributions and with typical values for the admixture coefficients [7, 37]

$$Q_{\Delta} = -b^2 \frac{4}{\sqrt{30}} \left( b_{S_S} b_{D_S} + \frac{2}{\sqrt{3}} b_{S'_S} b_{D_S} \right) e_{\Delta} = -0.087b^2 e_{\Delta}. \quad (42)$$

For  $b = 0.61$  fm one obtains then  $Q_{\Delta}^{imp} = -0.032 \text{fm}^2 e_{\Delta}$ . This has to be compared to our result  $Q_{\Delta}^{exc} = -0.119 \text{fm}^2 e_{\Delta}$ . Thus, in a more complete calculation we expect the corrections to eq.(39) coming from configuration mixing to be below some 30 %. In any case, our results clearly indicate that an eventual measurement of the quadrupole moment of the  $\Delta$  should not be interpreted in terms of an intrinsic deformation ( $D$ -waves) alone; it is more likely that quark-antiquark pair currents provide the dominant contribution to the quadrupole moment of the  $\Delta$ .

#### 4.2.2. $N \rightarrow \Delta$ transition quadrupole moment

Let us now turn to the  $N \rightarrow \Delta$  quadrupole transition moment. This observable and the related  $E2/M1$  ratio are exactly zero in the symmetric additive quark model [3]. The

inclusion of tensor forces due to one-gluon exchange between quarks leads to small  $D$ -state admixtures  $a_{D_M}$  ( $b_{D_S}, b_{D_M}$ ) in the nucleon ( $\Delta$ ) ground states wave functions of eq.(20) and to non-zero  $C2$  and  $E2$  transition amplitudes [7, 41]. The magnitude of this configuration mixing effect is, however, too small. Using the admixture coefficients of ref.[6] one obtains a transition quadrupole moment  $Q_{N \rightarrow \Delta}^{imp} = -0.0022 \text{ fm}^2$  calculated from the one-body spatial current density. A similar calculation using the one-body charge density and the admixture coefficients of ref. [37] gives  $Q_{N \rightarrow \Delta}^{imp} = -0.0195 \text{ fm}^2$  (for  $b = 0.613 \text{ fm}$ ). In any case, these values are much smaller than the empirical  $Q_{N \rightarrow \Delta}^{exp} = -0.0787 \text{ fm}^2$  (see sect. 4.5). Here, we show that the major part of the small  $C2$  transition amplitude is probably due to two-body pion and gluon exchange charge densities. This is analogous to the neutron charge radius and quadrupole moment discussed previously. Although all quarks in the  $N$  and the  $\Delta$  are assumed to be in  $S$ -states the system can absorb a  $C2$  or  $E2$  photon by simultaneously flipping the spin of *two quarks* (see fig.5). A glance at eq.(41) shows that the two-body charge operators can indeed induce such a  $\Delta S = 2$  transition. Using the total charge density of eq.(28) and having replaced the initial state by the nucleon wave function, we obtain from the  $q \rightarrow 0$  limit of eq.(38)

$$Q_{N \rightarrow \Delta} = -\frac{1}{\sqrt{2}} b^2 \frac{(\delta_g + \delta_\pi)}{3m_q} = -\frac{1}{\sqrt{2}} b^2 \left( \frac{M_\Delta - M_N}{M_N} \right) = \frac{1}{\sqrt{2}} r_n^2. \quad (43)$$

The corresponding numerical results are listed in table 4.

Eq.(43) relates the transition quadrupole moment to the neutron charge radius. As in eq.(39) no model parameter such as  $m_q$  or  $b$  appears in the final expression. We view this result as quite significant. It is almost needless to say that the simple result of eq.(43) will be modified in a more complete calculation including  $D$ -waves in the nucleon and  $\Delta$ . Nevertheless, we expect that eq.(43) captures the essential physics that makes both observables special and interesting: both  $r_n^2$  and  $Q_{N \rightarrow \Delta}$  are dominated by nonvalence quark degrees of freedom. Clearly, future experimental results must be carefully interpreted; the entire transition quadrupole moment *cannot* be attributed to the  $D$ -state admixtures in the  $N$  and  $\Delta$  ground state wave functions. The effect of two-body exchange currents must be taken into account, if one wants to isolate the effect of the quark-quark potential itself. If in a future experiment a  $N \rightarrow \Delta$  transition quadrupole moment of the order  $r_n^2/\sqrt{2}$  is confirmed it would most certainly be evidence for an important role of nonvalence quark degrees of freedom, i.e. pion and gluon exchange currents between quarks in this observable.

### 4.3. Magnetic moments

#### 4.3.1. Magnetic moments of the $\Delta$

The magnetic moments of the  $\Delta$  are defined as the  $q \rightarrow 0$  limit of the magnetic dipole form factor [38]

$$F_M(\mathbf{q}^2) = \frac{2\sqrt{6\pi}M_N}{iq} \langle JM_J=J TM_T | \frac{-i}{4\pi} \int d\Omega_q [Y^1(\hat{\mathbf{q}}) \times \mathbf{J}(\mathbf{q})]^1 | JM_J=J TM_T \rangle, \quad (44)$$

where  $\mathbf{J}$  is the total current operator in eq.(29). In the additive quark model one obtains (in units of nuclear magnetons ( $\mu_N = \frac{e}{2M_N}$ )):

$$\mu_\Delta = 3 e_\Delta. \quad (45)$$

Including two-body exchange currents, we have

$$\mu_{\Delta} = \left( 3 + \frac{2b^2}{3} M_N \delta_g(b) + \frac{3\delta\pi(b)}{2M_N} - \frac{6}{M_N} (V^{conf}(b) + V^{\sigma}(b)) \right) e_{\Delta}. \quad (46)$$

The first term in eq.(47) corresponds to the well-known single-quark current result  $\mu_{\Delta} = \mu_p e_{\Delta}$ . The remaining terms express the gluon, pion, and scalar exchange current contributions, through corresponding potential matrix elements. All contributions to the  $\Delta$  magnetic moments are proportional to the charge of the  $\Delta$ . Therefore, the  $\Delta^0$  magnetic moment is predicted to be zero. This is in agreement with the additive quark model as well as with a recent lattice calculation [49]. We list our numerical results in table 5. Note the large gluon contribution to the  $\Delta^{++}$  magnetic moment, which gets cancelled by a similarly large *scalar* exchange current correction.<sup>‡</sup> The cancellation of the gluon and confinement exchange currents is closely connected to the cancellation of spin-orbit forces in the gluon and confinement potentials [22]. For this cancellation it is essential that the condition  $M_N(b) = 3m_q = 939$  MeV be satisfied and that the harmonic oscillator parameter  $b \approx 1/m_q \approx 0.6$  fm be consistent with the neutron charge radius of eq.(35). Note that in the case of the  $\Delta$  elastic form factors, the dominant isovector pion pair and pionic exchange currents proportional to  $(\boldsymbol{\tau}_1 \times \boldsymbol{\tau}_2)_3$  do not contribute. Therefore, we have to include the next-to-leading order isovector pion pair-current in eq.(26), which is of the same order as the isoscalar pion pair-current. We then reproduce the general result [50] that the  $\Delta$  magnetic moments and radii are proportional to the charge of the  $\Delta$  given in eq.(37). In ref. [50] it has been argued that the pion contribution to the isoscalar nucleon magnetic moment used by Brown *et al.* [51] induces an intolerably large violation of this proportionality. Here, we show that if the isovector and isoscalar pion exchange currents are consistently calculated to the same nonrelativistic order, the proportionality of the  $\Delta$  magnetic moments to the charge of the  $\Delta$  holds even in the presence of pions.

Our result does not much deviate from the experimental value  $\mu_{\Delta^{++}} = 5.7 \pm 1.0 \mu_N$  [46] and is within the experimental range  $\mu_{\Delta^{++}} = 3.7 - 7.5 \mu_N$  given by the Particle Data Group [47]. However, it is larger than the most recent experimental value [48]. It should be mentioned that the determination of  $\mu_{\Delta^{++}}$  from  $\pi p \rightarrow \pi p \gamma$  bremsstrahlung experiments [48, 46] needs theoretical input from  $\pi N$  scattering models with  $\Delta$  degrees of freedom. Therefore, the extraction of the “bare”  $\Delta^{++}$  magnetic moment from the  $\pi p$  bremsstrahlung data has a certain model dependence that should not be underestimated. We also mention that quark model calculations, such as the one presented here neglect the coupling of the  $\Delta$  to the  $\pi N$  decay channel and thus predict “bare” electromagnetic moments. Our result for the  $\Delta^{++}$  magnetic moment agrees reasonably well with a chiral bag model calculation by Krivoruchenko [12].

For comparison and later use in the  $N \rightarrow \Delta$  transition moment, we give our results for the nucleon magnetic moments (in units of nuclear magnetons ( $\mu_N = \frac{e}{2M_N}$ )):

$$\begin{aligned} \mu_p &= 3 + \frac{b^2}{3} M_N \delta_g(b) + M_N \delta_{\pi}(b) \left( \frac{1}{4M_N^2} - \frac{b^2}{3} \right) - M_N \left( \left( \frac{1}{\mu^2} + \frac{1}{3} b^2 \right) \delta_{\pi\mu}(b) - (\mu \leftrightarrow \Lambda) \right) \\ &\quad - \frac{6}{M_N} (V^{conf}(b) + V^{\sigma}(b)) \\ \mu_n &= -2 - \frac{b^2}{9} M_N \delta_g(b) + M_N \delta_{\pi}(b) \left( \frac{1}{4M_N^2} + \frac{b^2}{3} \right) + M_N \left( \left( \frac{1}{\mu^2} + \frac{1}{3} b^2 \right) \delta_{\pi\mu}(b) - (\mu \leftrightarrow \Lambda) \right) \end{aligned}$$

<sup>‡</sup>A vector confinement current has the same sign as the one-gluon exchange current.



$$+ \frac{4}{M_N} \left( V^{conf}(b) + V^\sigma(b) \right). \quad (47)$$

The first term in eq.(47) corresponds to the well-known single-quark current result  $\mu_p = 3\mu_N$  and  $\mu_n = -2\mu_N$ . The other terms are the gluon pair, pion pair ( $\mu_{\pi q\bar{q}}$ ), pionic ( $\mu_{\gamma\pi\pi}$ ), and scalar exchange current contributions to the magnetic moments. In addition to the cancellation between gluon and confinement exchange currents, there is a substantial cancellation between the pion pair and pionic exchange currents. Consequently, the overall exchange current effect is about 5 – 10% of the impulse approximation result. We have previously shown that the cancellation between the pion pair and pionic currents only occurs if the  $\delta$ -function term in the one-pion exchange potential is included [22]. Recently, we have calculated the magnetic moments of the entire baryon octet including the exchange currents of fig.2. We find that the cancellations between various two-body currents also occur for the hyperon magnetic moments [23] provided that the quark core radius  $b \approx 1/m_q$ , which is consistent with the value required by the neutron charge radius of eq.(35).

#### 4.3.2. $N \rightarrow \Delta$ transition magnetic moment

Next we calculate the  $N \rightarrow \Delta$  magnetic transition moment. In contrast to the magnetic moments, where both isoscalar and isovector exchange currents contribute, only isovector currents contribute to the  $N \rightarrow \Delta$  transition magnetic moment. Using eq.(47) we can express our result for the transition moment as

$$\mu_{N \rightarrow \Delta} = \frac{2\sqrt{2}}{3} \left( \mu_{imp}^p + \frac{1}{2}\mu_{gq\bar{q}}^p + \frac{3}{2} \left( \mu_{\gamma\pi\pi}^{IV p} + \mu_{\pi q\bar{q}}^{IV p} \right) + \mu_\sigma^p + \mu_{conf}^p \right). \quad (48)$$

We obtain the numbers in the last two rows of table 5. We see that the total transition moment is about 13% lower than the impulse result. Again, there are substantial cancellations among the different terms. In particular, eq.(48) shows that there is the same cancellation between the pion pair and pionic contribution as in the nucleon magnetic moments. We point out that our analytic result for the total pion exchange current contribution to the transition magnetic moment,  $\mu_{N \rightarrow \Delta}^\pi = 0.176\mu_N$ , is somewhat larger than a recent phenomenological estimate, which gives  $\mu_{p \rightarrow \Delta^+}^\pi \approx 0.074\mu_N$  [52].

Finally, we would like to point out that the dominant contribution to the  $N \rightarrow \Delta$  transition magnetic moment comes from the single quark current, i.e. the first term in eq.(48). One can show that the impulse contribution is proportional to the overlap of the orbital symmetric nucleon and  $\Delta$  wave functions. This holds true even in the presence of configuration mixing provided that the  $D$ -state admixture is small. Therefore, any model in which this overlap is small, due to, for example, very different values of  $b$  in the nucleon and  $\Delta$  wave functions will give a very small value of the  $N \rightarrow \Delta$  transition moment.

We close this section by summarizing the main points. It has been known for some time that baryon magnetic moments are valence quark dominated. Our calculation explicitly shows that corrections coming from nonvalence quark degrees of freedom, such as exchange currents, are important but rarely exceed 15% of the additive quark model value. The problem with the underestimation of the  $N \rightarrow \Delta$  transition magnetic moment persists also after inclusion of exchange currents.

#### 4.4. Magnetic radii

Magnetic radii of hadrons measure the extension of the spatial current distribution. As the charge radii, they are interesting quantities which are quite sensitive to various model assumptions. The magnetic radius is defined as the slope of the magnetic form factor at zero momentum transfer:

$$r_M^2 = -\frac{6}{F_M(0)} \frac{d}{d\mathbf{q}^2} F_M(\mathbf{q}^2) \Big|_{\mathbf{q}^2=0}, \quad (49)$$

Analytic expressions for the magnetic radii of the nucleon, including exchange currents, were given previously [22]. Here, we list the results for the  $\Delta$  magnetic radii:

$$r_\Delta^2 = \frac{e_\Delta}{\mu_\Delta} \left\{ 3b^2 + \frac{11}{30} M_N b^4 \delta_g(b) + \frac{3}{20 M_N} b^2 \left( 10\delta_\pi(b) + \frac{3}{2} b \delta'_\pi(b) \right) - \frac{9}{M_N} b^2 V^{conf}(b) - \frac{3}{2 M_N} b^2 \left( 4V^\sigma(b) + b \frac{\partial}{\partial b} V^\sigma(b) \right) \right\} + r_{\gamma q}^2. \quad (50)$$

Likewise, we obtain for  $N \rightarrow \Delta$  magnetic transition radii:

$$r_{N \rightarrow \Delta}^2 = \frac{2\sqrt{2}}{\mu_{N \rightarrow \Delta}} \left\{ b^2 + \frac{11}{360} M_N b^4 \delta_g(b) - \frac{1}{60} M_N b^4 \left( 10\delta_\pi(b) + \frac{3}{2} b \delta'_\pi(b) \right) + \frac{1}{2} r_{\gamma\pi\pi}^2 \mu_p - \frac{3}{M_N} b^2 V^{conf}(b) - \frac{1}{2 M_N} b^2 \left( 4V^\sigma(b) + b \frac{\partial}{\partial b} V^\sigma(b) \right) \right\} + r_{\gamma q}^2. \quad (51)$$

Here,  $r_{\gamma\pi\pi}^2$  is the pionic current contribution to the proton magnetic radius [22] and  $\delta'_\pi(b) = \frac{\partial}{\partial b} \delta_\pi(b)$ .

As is clearly seen in table 6, the scalar exchange current cancels the effect of gluon and pion exchange currents to a large extent. Note that a vector-type confinement potential would have the same sign as the gluon contribution and would completely spoil the agreement obtained.

#### 4.5. The $\gamma + N \rightarrow \Delta$ helicity amplitudes

In this section we consider the helicity amplitudes for the transition  $\gamma + N \rightarrow \Delta$ . The transverse helicity amplitudes are defined as

$$\begin{aligned} A_{3/2} &= -e\sqrt{2\pi/\omega} \langle \Delta J_z = 3/2 | \boldsymbol{\epsilon} \cdot \mathbf{J} | N J_z = 1/2 \rangle \\ A_{1/2} &= -e\sqrt{2\pi/\omega} \langle \Delta J_z = 1/2 | \boldsymbol{\epsilon} \cdot \mathbf{J} | N J_z = -1/2 \rangle, \end{aligned} \quad (52)$$

where  $e^2 = 1/137$ . In table 7, we show our results for the transverse helicity amplitudes. For the  $N \rightarrow \Delta$  transition, only  $M1$  and  $E2$  multipoles contribute. In this paper we calculate the  $E2$  contribution from the charge density using Siegert's theorem, which relates the transverse electric multipoles to the Coulomb multipoles in the long wave-length limit. It was noted [8, 53] that a calculation of the  $E2$  multipole via the charge density is to be preferred. In addition to the reasons already mentioned in ref.[8, 53] there may be an even more important reason for this large discrepancy between a calculation based on the charge and spatial current density. We conjecture that the reason for the large difference

is that the former includes spatial exchange current corrections of spin-orbit type by virtue of Siegert's theorem while the latter does not. The issue deserves further study. In any case, the advantage of using Siegert's theorem clearly outweighs the error induced by using the long wave-length limit in a situation which involves a substantial momentum transfer of  $q \approx M_\Delta - M_N$ . The relation between the multipole form factors and the helicity amplitudes is in the center of mass frame [37]

$$\begin{aligned} A_{3/2}(\mathbf{q}^2) &= -\sqrt{3\pi\omega} \left( \frac{e}{2M_N} \right) \left( F_M^{N \rightarrow \Delta}(\mathbf{q}^2) - \frac{M_N\omega}{6} F_Q^{N \rightarrow \Delta}(\mathbf{q}^2) \right) \\ A_{1/2}(\mathbf{q}^2) &= -\sqrt{\pi\omega} \left( \frac{e}{2M_N} \right) \left( F_M^{N \rightarrow \Delta}(\mathbf{q}^2) + 3 \frac{M_N\omega}{6} F_Q^{N \rightarrow \Delta}(\mathbf{q}^2) \right), \end{aligned} \quad (53)$$

where  $F_M$  and  $F_Q$  are the magnetic and quadrupole transition form factors, which are normalized to the magnetic (sect. 4.4) and quadrupole (sect. 4.2) transition moments. The relation between our  $F_M^{N \rightarrow \Delta}$  and  $F_Q^{N \rightarrow \Delta}$  and Giannini's [37] dimensionless  $G_{M1}$  and  $G_{E2}$  is:  $G_{M1} = (\sqrt{6}/2) F_M^{N \rightarrow \Delta}$  and  $G_{E2} = -(\omega M_N \sqrt{6}/12) F_Q^{N \rightarrow \Delta}$ . The origin of the factors multiplying the magnetic and quadrupole form factors in eq.(53) is explained in ref. [17].

There have been previous calculations of two-body current contributions to the  $N \rightarrow \Delta$  transition in the CQM, but not for the  $\Delta$  electromagnetic moments and radii. Ohta [55], calculates two-body currents resulting from minimal substitution in the one-gluon exchange and a scalar confinement potential as well as relativistic corrections to the single-quark current but does not consider pion exchange currents. In this early calculation, large anomalous magnetic moments for the quarks  $\kappa = 1.83$  were used. This leads to an unconventional non-relativistic impulse result  $A_{3/2}(NRI) = -505 \cdot 10^{-3} \text{ GeV}^{-1/2}$  which is drastically reduced by large relativistic corrections to the single-quark current,  $A_{3/2}(RCI) = 97 \cdot 10^{-3} \text{ GeV}^{-1/2}$ , and an even larger contribution of the two-body currents,  $A_{3/2}(EXC) = 189 \cdot 10^{-3} \text{ GeV}^{-1/2}$ . However, large anomalous magnetic moments for the constituent quarks are in conflict with general current algebra arguments [31] and with explicit calculations in the Nambu-Jona-Lasinio model [34].

Robson [19] has included the pion pair and pionic exchange currents resulting from minimal substitution in the one-pion exchange potential but ignores gluons. He finds that the pionic current is small and neglects this contribution. In contrast, our calculation shows that the pionic current is big and negative. It completely cancels the positive pion pair-current. The total pion contribution has thus the same sign as the impulse result. This cancellation between pion pair and pionic currents is closely connected with a similar cancellation in the nucleon magnetic moments [22] (see also table 5). Another difference is that in ref. [19] the  $E2$  contribution to the helicity amplitudes has been neglected. However, it is in the  $E2$  amplitude where the exchange currents are most clearly seen.

Finally, we give our result for the  $E2/M1$  ratio using the definition of Kumano [12]

$$\frac{E2}{M1} = \frac{1}{3} \frac{A_{1/2}(E2)}{A_{1/2}(M1)} = \frac{\omega M_N}{6} \frac{Q_{N \rightarrow \Delta}}{\mu_{N \rightarrow \Delta}} = -0.035. \quad (54)$$

Our predicted  $E2/M1$  ratio is somewhat larger than the recent experimental value extracted from photo-pionproduction at MAMI in Mainz which gives  $(E2/M1)_{exp} = -0.025 \pm 0.002$  [56]. The LEGS-BNL data (see, for example, the article by D'Angelo in ref.[1]) seem to favor a larger  $(E2/M1)_{exp} = -0.03$ . Comparing with other theoretical predictions, our result agrees well with Skyrme model results,  $E2/M1 \simeq -(0.02 - 0.05)$  [17] and  $E2/M1 = -0.037$

[18] and dynamical models for photo-pionproduction  $E2/M1 = -0.031$  [16]. Note that our  $E2$  amplitude  $G_{E2}(0) = -\frac{\omega M_N \sqrt{6}}{12} Q_{N \rightarrow \Delta} = 0.105$  compares reasonably well with the phenomenological analysis of Devenish *et al.* [57], which gives  $G_{E2}(0) = 0.02 G_{M1}(0) \approx 0.1$  [37]. Our prediction is based on the parameter-free result of eq.(43) which relates the transition quadrupole moment to the neutron charge radius.

Very recently, there has been a new determination of the  $E2/M1$  ratio, applying the speed plot technique to fixed- $t$  dispersion relations for the photo-pionproduction amplitudes. The authors include new photo-pionproduction data from the continuous electron beam facilities in Mainz and Bonn. They obtain  $E2/M1 = -0.035$  [58] in excellent agreement with our quark model prediction including exchange currents. <sup>§</sup>However, several caveats are in order here. First, the inclusion of configuration mixing would certainly modify the numerical value for this ratio. Second, we underestimate the empirical  $N \rightarrow \Delta$  transition magnetic moment. Third, the extraction of a  $\gamma N \rightarrow \Delta$  photocoupling from the photo-pionproduction data is not model-independent and it would be much safer to calculate the complete photo pionproduction multipoles before comparing with experiment [59]. Nevertheless, our prediction of a *large*  $E2/M1$  ratio emphasizes the important role of nonvalence quark degrees of freedom in the transition quadrupole moment, irrespective of whether one refers to them as meson cloud of the nucleon, sea-quark degrees of freedom, or exchange currents.

Next, we show in fig.6 the four-momentum dependence of the helicity amplitudes. We observe that exchange currents contribute to the  $A_{3/2}$  amplitude between 7% at  $Q^2 = 0$  and 19% of the impulse result at  $Q^2 = 0.5 \text{ GeV}^2$ . The small value at  $Q^2 = 0$  is firstly due to cancellations of different exchange current contributions to  $F_M^{N \rightarrow \Delta}$ . Secondly, the exchange current contributions to  $F_M^{N \rightarrow \Delta}$  and  $F_Q^{N \rightarrow \Delta}$  form factors interfere destructively in the  $A_{3/2}$  amplitude (see also table 7). On the other hand, in the  $A_{1/2}$  amplitude the exchange current dominated  $F_Q^{N \rightarrow \Delta}$  form factor enters with an additional weight factor of three and the exchange current contributions to  $F_M^{N \rightarrow \Delta}$  and  $F_Q^{N \rightarrow \Delta}$  form factors interfere constructively. Therefore, for small momentum transfers the  $A_{1/2}$  helicity amplitude is appreciably influenced by exchange currents. For example, at  $Q^2 = 0$  their contribution is 27% of the impulse result.

Finally, with respect to the helicity amplitudes of other resonances, we have recently calculated their effect for the  $M1$  excitation of the Roper resonance [60]. In this case, the inclusion of exchange currents gives for both the proton and neutron an encouraging agreement with the empirical values for the  $A_{1/2}$  amplitudes. More work is needed to systematically study the effect of exchange currents in the photocouplings of higher resonances.

## 5. Summary

In summary, the interaction between quarks manifests itself not only in various two-body potentials, but also in corresponding two-body corrections to the electromagnetic current operator. These must be included if the total current is to be conserved. The exchange current operators describe the coupling of the photon to nonvalence degrees of freedom (e.g. quark-antiquark pairs) not included in the mass, size, and wave function of the constituent quarks. We have pointed out that most previous calculations of electromagnetic properties

---

<sup>§</sup>If we use  $\mu_{N \rightarrow \Delta} \approx 4\mu_N$  as the empirical value for the transition magnetic moment we obtain  $E2/M1 = -0.022$ .

built on free quark currents are incomplete because they violate current conservation even in lowest order.

In the present paper we have calculated the electromagnetic radii and moments of the nucleon and the  $\Delta$ -isobar, as well as the corresponding transition radii and moments in the nonrelativistic quark model. Our main purpose was to study to what extent the theoretical predictions for these observables are modified by the inclusion of the leading order relativistic corrections of *two-body nature* in the electromagnetic current. All observables were calculated with a single set of parameters in order to see how the different two-body currents affect various observables. Our numerical results clearly show the importance of individual exchange current contributions.

With respect to the magnetic moments we found that although individual exchange current corrections can be quite large, their overall effect typically changes the additive quark model result by less than 15%. This clearly shows that magnetic moments are to a large extent valence quark dominated. In particular, for the  $N \rightarrow \Delta$  transition magnetic moment, a large discrepancy between our theoretical prediction and the experimental result is left unexplained even after inclusion of exchange currents.

In the case of quadrupole moments, we have shown that even if there is no explicit  $D$ -state admixture in the  $\Delta$  wave function, one still obtains a large contribution to the  $\Delta$  quadrupole moment and to the corresponding  $N \rightarrow \Delta$  transition quadrupole moment due to two-body pion and gluon exchange currents. This is depicted in Fig.5 where an  $E2(C2)$  photon can be absorbed on a correlated quark pair even if all three quarks in the nucleon are in  $S$ -states. Without two-body exchange currents the  $E2(C2)$  amplitude would be exactly zero in the present approximation, which neglects configuration mixing. Configuration mixing alone is too small to explain the empirical  $E2(C2)$  amplitude. We find that the  $E2(C2)$  transition to the  $\Delta$  is mainly a *two-body* process involving the simultaneous spin-flip of two quarks.

We have, based on the inclusion of exchange currents, derived a number of analytic relations between the  $\Delta - N$  mass splitting and the electromagnetic observables of the  $\Delta - N$  system; in particular, our eqs.(39,43) suggest that the quadrupole moment of the  $\Delta$  and the  $N \rightarrow \Delta$  transition quadrupole moment are closely related to the neutron charge radius, which, in turn, is related to the quark core size of the nucleon and the  $\Delta - N$  mass difference according to eq.(35). Because these relations are derived for pure  $S$ -wave functions they can only be approximately valid. We have previously shown [21] that a more consistent calculation including both configuration mixing and exchange currents leads to deviations of some 10 – 20% between, for example, the prediction of eq.(35) and the total result including configuration mixing. Therefore, eqs.(35,39,43) are very useful. First, the numerical estimates, e.g. for the neutron charge radius are in excellent agreement with experiment, and although there is no experimental information on the  $\Delta$  quadrupole moment, previous and very recent extractions of the transition quadrupole moment indicate a value consistent with the prediction of eq.(43). Second, they seem to correctly describe the underlying physics common to these observables:  $r_n^2$ ,  $Q_\Delta$  and  $Q_{N \rightarrow \Delta}$  are almost exclusively dominated by non-valence quark degrees of freedom. Third, these relations make the underlying connection between the excitation spectrum of the nucleon (potentials) and electromagnetic properties (two-body currents) explicit. We cannot resist the temptation to speculate whether eqs.(39, 43) are of a somewhat more general validity than their derivation would suggest.

Our prediction for the  $E2/M1$  ratio, which is based on our analytic expressions for  $Q_{N \rightarrow \Delta}$  and  $\mu_{N \rightarrow \Delta}$  results in  $E2/M1 = -0.035$ . This value is significantly larger than the value estimated by the Particle Data Group [47] but is consistent with a recent reanalysis of

photo-pionproduction data from several experiments [58]. If we use the empirical value for the  $\mu_\Delta$  we obtain  $E2/M1 = -0.022$  in agreement with the recent Mainz experiment [56].

Clearly, there are a number of other effects, such as configuration mixing, relativistic boost corrections, small anomalous magnetic moments of the quarks, strangeness content of the nucleon and  $\Delta$ , etc. that should be included in a more detailed analysis. Nevertheless, it is safe to conclude that the residual spin-dependent interactions manifest themselves not only in excited state admixtures to ground state wave functions but also in the form of two-body exchange currents between quarks. Exchange currents must be included in the theoretical interpretation of experimental results before one can draw conclusions about details of the quark-quark interaction. In particular, we find that the  $E2$ -amplitude, in photo-pionproduction is predominantly a *two-quark spin-flip transition*; it is to a much lesser extent a consequence of small  $D$ -states in the nucleon. Hence, the experimental confirmation of a large  $E2$ -amplitude in the  $N \rightarrow \Delta$  transition would be evidence for pion and gluon exchange currents between quarks.

**Acknowledgement:** We thank Andreas Wirzba for useful correspondence.

## References

- [1] For a recent review see: *Progr. Part. Nucl. Phys.* **34** (1995), ed. Amand Faessler
- [2] M. A. B. Bég, B. W. Lee, and A. Pais, *Phys. Rev. Lett.* **13** (1964) 514
- [3] C. Becchi and G. Morpurgo, *Phys. Lett.* **17** (1965) 352
- [4] R. H. Dalitz and D. G. Sutherland, *Phys. Rev.* **146** (1966) 1180
- [5] Frank Kalleicher, PhD thesis, University of Mainz, (1993)
- [6] R. Koniuk and N. Isgur, *Phys. Rev.* **D21** (1980) 1868
- [7] S. S. Gershtein and G. V. Dzhikiya, *Sov. J. Nuc. Phys.* **34** (1982) 870
- [8] D. Drechsel and M. M. Giannini, *Phys. Lett.* **B143** (1984) 329
- [9] F. E. Close, Z. P. Li, *Phys. Rev.* **D42** (1990) 2194
- [10] M. Warns, H. Schröder, W. Pfeil, H. Rollnik, *Z. Phys.* **C45** (1990) 627
- [11] S. Capstick, *Phys. Rev.* **D46** (1992) 2864
- [12] S. Kumano, *Phys. Lett.* **B214** (1988) 13; K. Bermuth, D. Drechsel, L. Tiator, and J. B. Seaborn, *Phys. Rev.* **D37** (1988) 89; I. Guiasu and R. Koniuk, *Phys. Rev.* **D36** (1987) 2757; M. Weyrauch, *Phys. Rev.* **D35** (1987) 1574; M. I. Krivoruchenko, *Sov. J. Nucl. Phys.* **45** (1987) 109.
- [13] R. M. Davidson, N. C. Mukhopadhyay, and R. S. Wittman, *Phys. Rev.* **D43** (1991) 71
- [14] P. Christillin and G. Dillon, *J. Phys.* **G18** (1992) 1915
- [15] J. M. Laget, *Nucl. Phys.* **A481** (1988) 765
- [16] S. Nozawa, B. Blankleider, and T.-S.H. Lee, *Nucl. Phys.* **A513** (1990) 459
- [17] A. Wirzba and W. Weise, *Phys. Lett.* **B188** (1987) 6
- [18] A. Abada, H. Weigel and Hugo Reinhardt, *Phys. Lett* **366** (1996) 26
- [19] D. Robson, *Nucl. Phys.* **A560** (1993) 389
- [20] M. Weyrauch and H. J. Weber, *Phys. Lett.* **B171** (1986) 13
- [21] A. Buchmann, E. Hernández, and K. Yazaki, *Phys. Lett.* **B269** (1991) 35
- [22] A. Buchmann, E. Hernández, and K. Yazaki, *Nucl. Phys.* **A569** (1994) 661
- [23] Georg Wagner, A. J. Buchmann, and Amand Faessler, *Phys. Lett.* **B359** (1995) 288
- [24] E. Shuryak, *Phys. Rep.* **115** (1984) 151
- [25] for recent reviews see: W. Lucha, F. F. Schöberl, D. Gromes, *Phys. Rep.* **200** (1991) 127
- [26] A. De Rujula, Howard Georgi, and S. L. Glashow, *Phys. Rev.* **D12** (1975) 147
- [27] M. Kirchbach, *Czech. J. Phys.* **43** (1993) 319; G. Ecker, *Czech. J. Phys.* **44** (1994) 405
- [28] A. Manohar and H. Georgi, *Nucl. Phys.* **B234** (1984) 189

- [29] K. Shimizu, Phys. Lett. **B148** (1984) 418; K. Maltman, Nucl. Phys. **A446** (1985) 623; D. Robson, Phys. Rev. **D35** (1985) 1029; K. Bräuer, A. Faessler, F. Fernandez and K. Shimizu, Z. Phys. **A320** (1985) 609; F. Fernandez and E. Oset, Nucl. Phys. **A455** (1986) 720
- [30] I. T. Obukhovskiy and A. M. Kusainov, Phys. Lett. **B238** (1990) 142; F. Fernandez, A. Valcarce, U. Straub and A. Faessler, J. Phys. **G19** (1993) 2013; A. Valcarce, A. Buchmann, F. Fernandez, and A. Faessler, Phys. Rev. **C50** (1994) 2246
- [31] Steven Weinberg, Phys. Rev. Lett. **65** (1990) 1181
- [32] V. A. Petrunin, Sov. J. Part. Nucl. **12** (1981) 278
- [33] D. P. Stanley and D. Robson, Phys. Rev. **D26** (1982) 223
- [34] U. Vogl, M. Lutz, S. Klimt and W. Weise, Nucl. Phys. **A516** (1990) 469
- [35] H. J. Weber, and H. Arenhövel, Phys. Rep. **36** (1978) 277
- [36] H. F. Jones and M. D. Scadron, Ann. Phys. **81** (1973) 1
- [37] M. M. Giannini, Rep. Prog. Phys. **54** (1990) 453
- [38] M. Gari and H. Hyuga, Nucl. Phys. **A264** (1976) 409
- [39] C. Gobbi, S. Boffi, and D. O. Riska, Nucl. Phys. **A547** (1992) 633
- [40] R. D. Carlitz, S. D. Ellis, and R. Savit, Phys. Lett. **B68** (1977) 443
- [41] N. Isgur and G. Karl, and R. Koniuk, Phys. Rev. **D25** (1982) 2394
- [42] A. Buchmann, Y. Yamauchi, and A. Faessler, Nucl. Phys. **A496** (1989) 621.
- [43] G. G. Simon, F. Borkowski, Ch. Schmitt and V. H. Walther, Z. Naturf. **35a** (1980) 1
- [44] Chr. V. Christov et al, Progr. Part. Nucl. Phys. **37** (1996) 91
- [45] M. I. Krivoruchenko and M. M. Giannini, Phys. Rev. **D43** (1991) 3763
- [46] B. M. K. Nefkens, Phys. Rev. **D18** (1978) 3911; P. Pascual and R. Tarrach, Nucl. Phys. **B134** (1978) 133
- [47] Particle Data Group, Phys. Rev. **D50** (1994) 1173
- [48] A. Bosshard et al., Phys. Rev. **D44** (1991) 1962
- [49] D. B. Leinweber, T. Draper and R. M. Woloshyn, Phys. Rev. **D46** (1992) 3067
- [50] G. Dillon, G. Morpurgo, Z. Phys. **C62** (1994) 31
- [51] G. E. Brown, M. Rho, and V. Vento, Phys. Lett. **B97** (1980) 423
- [52] L. Ya. Glozman and D. O. Riska, Phys. Rep. **268** (1996) 263
- [53] M. Bourdeau and N. C. Mukhopadhyay, Phys. Rev. Lett. **58** (1987) 976
- [54] H. Tanabe and K. Ohta, Phys. Rev. **C31** (1985) 1876
- [55] K. Ohta, Phys. Rev. Lett. **43** (1979) 1201
- [56] G. Beck, Proc. Int. Conf. Baryons 95, Santa Fé (1995)



- [57] R. C. E. Devenish, T. S. Eisenschitz and J. G. Körner, Phys. Rev. **D14** (1976) 3063.
- [58] O. Hanstein, D. Drechsel and L. Tiator, nucl-th/9605008
- [59] P. Wilhelm, Th. Wilbois, and H. Arenhövel, preprint, University of Mainz, MKPH-T-96-1
- [60] A. J. Buchmann, U. Meyer, E. Hernández, Amand Faessler, Proceedings of Mesons 96, May 10-14, Cracow, to be published in Acta Phys. Pol. (1996)

Table 1: Quark model parameters.

|          |            |                               |                  |                     |                               |
|----------|------------|-------------------------------|------------------|---------------------|-------------------------------|
| $b$ [fm] | $\alpha_s$ | $a_c$ [MeV fm <sup>-2</sup> ] | $m_\sigma$ [MeV] | $g_\sigma^2/(4\pi)$ | $\Lambda$ [fm <sup>-1</sup> ] |
| 0.613    | 1.093      | 20.20                         | 675              | 0.554               | 4.2                           |

Table 2: Contribution of the kinetic energy (without the rest mass term) and individual potential terms in the Hamiltonian to the nucleon mass of eq.(12) and the gluon ( $\delta_g$ ) and pion ( $\delta_\pi$ ) contributions to the  $\Delta - N$  mass splitting of eq.(16).  $cc$ : color Coulomb part of  $V^{OGEP}$ ,  $\delta$ :  $\delta$ -function part of  $V^{OGEP}$ . All entries are in [MeV].

| Term | $T^{kin}$ | $V^{conf}$ | $V_{cc}^{OGEP}$ | $V_\delta^{OGEP}$ | $V^\pi$ | $V^\sigma$ | Total | $\delta_g$ | $\delta_\pi$ |
|------|-----------|------------|-----------------|-------------------|---------|------------|-------|------------|--------------|
|      | 496.6     | 182.2      | -561.2          | 49.5              | -118.9  | -48.1      | 0.0   | 197.9      | 95.1         |

Table 3: Nucleon and  $\Delta(1232)$  charge radii including two-body exchange currents; i: impulse; g: gluon;  $\pi$ : pion;  $\sigma$ :  $\sigma$ -meson; c: confinement; t: total=impulse + gluon + pion + sigma + confinement. A finite electromagnetic quark size  $r_{\gamma q}^2 = 0.36$  fm<sup>2</sup> is used. The experimental proton and neutron charge radii are  $r_p = 0.862 \pm 0.012$  fm and  $\sqrt{|r_n^2|} = 0.345 \pm 0.003$  fm, respectively [43]. The charge radius of the  $\Delta^0$  is zero in the present model. All entries are in [fm<sup>2</sup>] except for the total result which is in [fm].

|          | $r_i^2$ | $r_g^2$ | $r_\pi^2$ | $r_\sigma^2$ | $r_c^2$ | $\sqrt{ r_t^2 }$ |
|----------|---------|---------|-----------|--------------|---------|------------------|
| $p$      | 0.736   | 0.119   | -0.057    | 0.041        | -0.174  | 0.815            |
| $n$      | 0.000   | -0.079  | -0.038    | 0.000        | 0.000   | 0.342            |
| $\Delta$ | 0.736   | 0.198   | -0.019    | 0.041        | -0.174  | 0.884            |

Table 4:  $\Delta(1232)$  quadrupole moments and  $N \rightarrow \Delta$  transition quadrupole moments, including two-body exchange currents; i: impulse; g: gluon;  $\pi$ : pion;  $\sigma$ :  $\sigma$ -meson; c: confinement; t: total=impulse + gluon + pion +sigma +conf. As in the neutron charge radius, spin-independent scalar exchange currents do not contribute to the  $\Delta$  quadrupole moments. The quadrupole moment of the  $\Delta^0$  is zero in the present model. The experimental values for the transition quadrupole moment are:  $Q_{N \rightarrow \Delta} = -0.0439 \text{ fm}^2$  using the empirical values for the helicity amplitudes [47];  $Q_{N \rightarrow \Delta} = -0.0787 \text{ fm}^2$  using the phenomenological analysis of ref.[57]; a recent Mainz analysis favors an even larger value  $Q_{N \rightarrow \Delta} = -0.1109 \text{ fm}^2$  [58]. All entries are in [ $\text{fm}^2$ ].

|                          | $Q_i$ | $Q_g$  | $Q_\pi$ | $Q_\sigma$ | $Q_c$ | $Q_t$  |
|--------------------------|-------|--------|---------|------------|-------|--------|
| $\Delta^{++}$            | 0.000 | -0.158 | -0.0761 | 0.000      | 0.000 | -0.234 |
| $\Delta^+$               | 0.000 | -0.079 | -0.038  | 0.000      | 0.000 | -0.117 |
| $\Delta^0$               | 0.000 | 0.000  | 0.000   | 0.000      | 0.000 | 0.000  |
| $\Delta^-$               | 0.000 | 0.079  | 0.038   | 0.000      | 0.000 | 0.117  |
| $p \rightarrow \Delta^+$ | 0.000 | -0.056 | -0.027  | 0.000      | 0.000 | -0.083 |
| $n \rightarrow \Delta^0$ | 0.000 | -0.056 | -0.027  | 0.000      | 0.000 | -0.083 |

Table 5: Nucleon and  $\Delta(1232)$  magnetic moments, and  $N \rightarrow \Delta$  transition magnetic moments including two-body exchange currents; i: impulse; g: gluon;  $\pi$ : pion;  $\sigma$ :  $\sigma$ -meson; c: confinement; t: total=impulse + gluon + pion + sigma + confinement. The contribution of the pion pair ( $\pi q \bar{q}$ ) and the pionic ( $\gamma \pi \pi$ ) currents are separately listed. The experimental proton and neutron magnetic moments are  $\mu_p = 2.792847386(63) \mu_N$  and  $\mu_n = -1.91304275(45) \mu_N$ , respectively [47]. The experimental range for the  $\Delta^{++}$  magnetic moment is  $\mu_{\Delta^{++}} = 3.7 - 7.5 \mu_N$  [47]. An older value is  $\mu_{\Delta^{++}} = 5.7 \pm 1.0 \mu_N$  [46] while the most recent value is  $\mu_{\Delta^{++}} = 4.52 \pm 0.50 \mu_N$  [48]. The experimental value for the  $N \rightarrow \Delta$  transition magnetic moment is  $\mu_{p \rightarrow \Delta^+} \approx 4.0 \mu_N$  [37]. All entries are in  $\mu_N$ .

|                          | $\mu_i$ | $\mu_g$ | $\mu_{\pi q \bar{q}}$ | $\mu_{\gamma \pi \pi}$ | $\mu_\sigma$ | $\mu_c$ | $\mu_t$ |
|--------------------------|---------|---------|-----------------------|------------------------|--------------|---------|---------|
| $p$                      | 3.000   | 0.598   | -0.262                | 0.411                  | 0.308        | -1.164  | 2.890   |
| $n$                      | -2.000  | -0.199  | 0.313                 | -0.411                 | -0.205       | 0.776   | -1.726  |
| $\Delta^{++}$            | 6.000   | 2.391   | 0.304                 | 0.000                  | 0.615        | -2.328  | 6.981   |
| $\Delta^+$               | 3.000   | 1.195   | 0.152                 | 0.000                  | 0.308        | -1.164  | 3.491   |
| $\Delta^0$               | 0.000   | 0.000   | 0.000                 | 0.000                  | 0.000        | 0.000   | 0.000   |
| $\Delta^-$               | -3.000  | -1.195  | -0.152                | 0.000                  | -0.308       | 1.164   | -3.491  |
| $p \rightarrow \Delta^+$ | 2.828   | 0.282   | -0.406                | 0.582                  | 0.290        | -1.098  | 2.477   |
| $n \rightarrow \Delta^0$ | 2.828   | 0.282   | -0.406                | 0.582                  | 0.290        | -1.098  | 2.477   |

Table 6: Magnetic radii of the nucleon and  $\Delta(1232)$  including two-body exchange currents; i: impulse; g: gluon;  $\pi$ : pion;  $\sigma$ :  $\sigma$ -meson; c: confinement; t: total=impulse + gluon + pion + sigma + confinement. The contribution of the pion pair ( $\pi q\bar{q}$ ) current and the pionic current ( $\gamma\pi\pi$ ) are listed separately. The magnetic radius of the  $\Delta^0$  is zero. A finite electromagnetic quark size,  $r_{\gamma q}^2 = 0.36 \text{ fm}^2$ , is used. The experimental proton and neutron magnetic radii are  $r_p^2 = 0.858 \pm 0.056 \text{ fm}$  and  $r_n^2 = 0.876 \pm 0.070 \text{ fm}$  [43]. All entries are in  $[\text{fm}^2]$ , except for total results which are in  $[\text{fm}]$ .

|                          | $r_i^2$ | $r_g^2$ | $r_{\pi q\bar{q}}^2$ | $r_{\gamma\pi\pi}^2$ | $r_\sigma^2$ | $r_c^2$ | $\sqrt{ r_t^2 }$ |
|--------------------------|---------|---------|----------------------|----------------------|--------------|---------|------------------|
| $p$                      | 0.764   | 0.117   | -0.053               | 0.185                | 0.058        | -0.372  | 0.836            |
| $n$                      | 0.852   | 0.065   | -0.105               | 0.309                | 0.065        | -0.415  | 0.878            |
| $\Delta$                 | 0.632   | 0.194   | 0.025                | 0.000                | 0.048        | -0.308  | 0.769            |
| $p \rightarrow \Delta^+$ | 0.840   | 0.064   | -0.096               | 0.305                | 0.064        | -0.409  | 0.876            |

Table 7: The  $A_{3/2}$  and  $A_{1/2}$  helicity amplitudes for the process  $\gamma + N \rightarrow \Delta(1232)$ , including two-body exchange currents; i: impulse; g: gluon;  $\pi q\bar{q}$ : pion pair;  $\gamma\pi\pi$ : pionic;  $\sigma$ :  $\sigma$ -meson; c: confinement; t: total=impulse + gluon + pion +sigma +conf. The  $M1$  and  $E2$  parts of the helicity amplitudes as well as their sum are listed. The experimental helicity amplitudes are  $A_{3/2} = -257 \pm 8$  and  $A_{1/2} = -141 \pm 5$  [47]. A previous analysis gave  $A_{1/2} = -84 \pm 5$  [54]. Our results are given at  $\mathbf{q}^2 = 0$ . All entries are given in standard units of  $[10^{-3} \text{ GeV}^{-1/2}]$ .

|  | $A_i$  | $A_g$ | $A_{\pi q\bar{q}}$ | $A_{\gamma\pi\pi}$ | $A_\sigma$ | $A_c$ | $A_t$  | $A_{exp}$ |
|--|--------|-------|--------------------|--------------------|------------|-------|--------|-----------|
| $A_{p \rightarrow \Delta^+}^{3/2}(M1)$ | -200.7 | -20.0 | 28.8               | -41.3              | -20.6      | 77.9  | -175.8 | -253.8    |
| $A_{p \rightarrow \Delta^+}^{3/2}(E2)$ | 0.0    | -4.1  | -2.0               | 0.0                | 0.0        | 0.0   | -6.1   | -3.2      |
| $A_{p \rightarrow \Delta^+}^{3/2}(T)$  | -200.7 | -24.1 | 26.8               | -41.3              | -20.6      | 77.9  | -181.9 | -257.0    |
| $A_{p \rightarrow \Delta^+}^{1/2}(M1)$ | -115.9 | -11.5 | 16.7               | -23.8              | -11.9      | 45.0  | -101.5 | -146.5    |
| $A_{p \rightarrow \Delta^+}^{1/2}(E2)$ | 0.0    | 7.1   | 3.4                | 0.0                | 0.0        | 0.0   | 10.5   | 5.5       |
| $A_{p \rightarrow \Delta^+}^{1/2}(T)$  | -115.9 | -4.4  | 20.1               | -23.8              | -11.9      | 45.0  | -90.9  | -141.0    |

## FIGURE CAPTIONS

Fig.1 Residual (a) one-gluon, (b) one-pion, and (c) one-sigma exchange potentials between constituent quarks. The hadronic size  $r_q$  of the constituent quarks is indicated by small dots.

Fig.2 One-body and two-body exchange currents between quarks: (a) impulse, (b) gluon pair, (c) pion pair, (d) pionic, (e) scalar pair. The finite electromagnetic size of the constituent quarks and the pion is indicated by the filled circles.

Fig.3 Pion loop contribution to the electromagnetic form factor of the constituent quarks. Vector meson dominance relates the finite electromagnetic size of the constituent quarks to the vector meson mass  $r_{\gamma q}^2 \approx 6/m_\rho^2$  [34].

Fig.4 One-body and two-body contributions to the quadrupole moment of the  $\Delta$  and to the  $N \rightarrow \Delta$  transition quadrupole moment. In diagram (a) the photon is absorbed on a single quark which remains in a positive energy state after the absorption of the photon. The dominant contribution of this diagram is obtained by sandwiching the standard *one-body* current between baryon wave functions. These wave functions must contain a tensor force induced *D*-state in order that the system can absorb a *C2* or *E2* photon through a *single-quark* transition. In diagram (b) the photon couples to a quark-antiquark pair in the baryon and the system can absorb a *C2* or *E2* photon on *two quarks*, even if all quarks are in *S*-states. This contribution is effectively described by the *two-body* exchange charge operators. Similar diagrams can be drawn for pion-exchange between quarks.

Fig.5 Pion and gluon exchange current contribution to the *E2* transition form factor. A major part of the *E2* transition form factor is due to photon absorption on a correlated pair of quarks, interacting via gluon and pion exchange. The *E2* photon simultaneously flips the spin of *two quarks* in the nucleon leading to the  $\Delta(1232)$ . This process is more important than the one where an *E2* photon is absorbed on a single-quark moving in a *D*-wave (see fig. 4a).

Fig.6 The  $A_{1/2}(Q^2)$  (a) and  $A_{3/2}(Q^2)$  (b) helicity amplitudes as a function of the four-momentum transfer  $Q$ . Here, we keep  $\omega_{cm} = 258$  MeV fixed and vary the three-momentum transfer  $\mathbf{q}$ . The individual two-body exchange current contributions are shown separately.

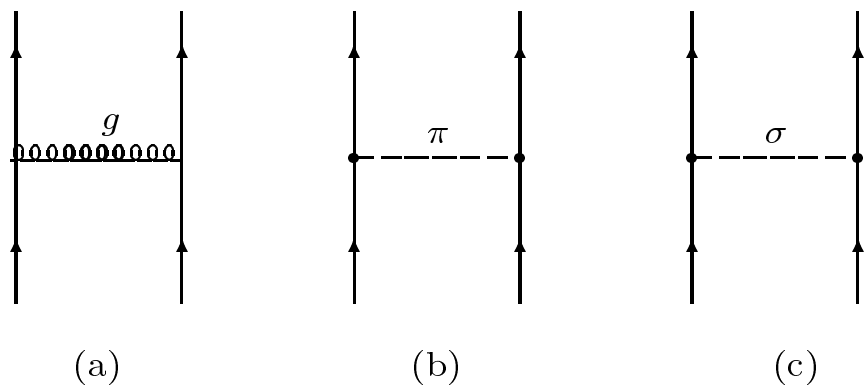


Figure 1:

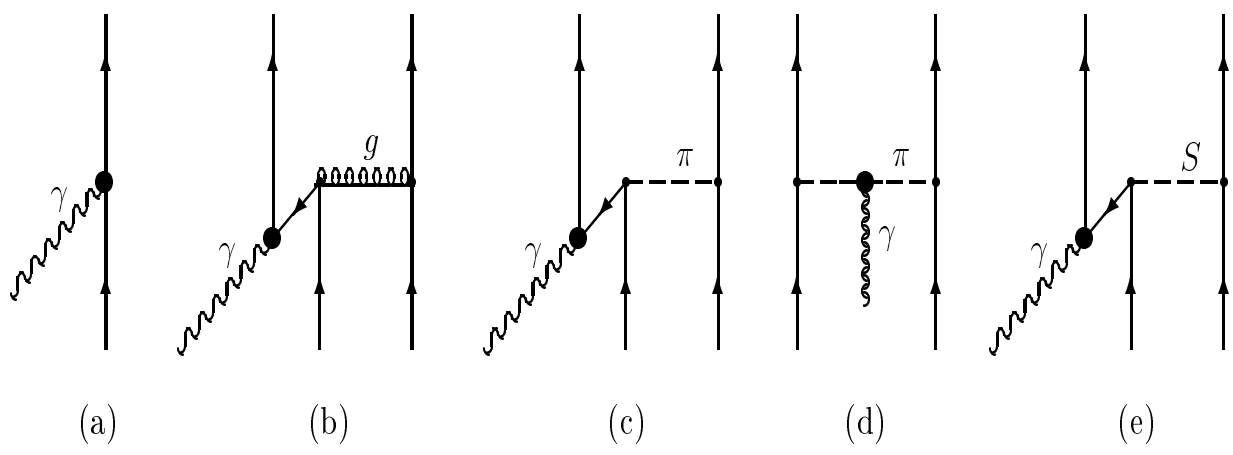


Figure 2:

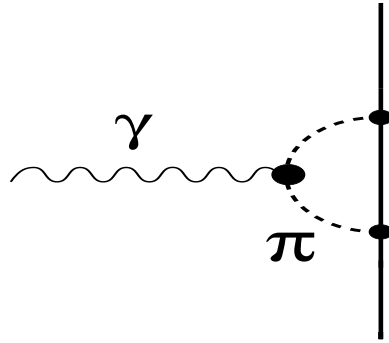


Figure 3:

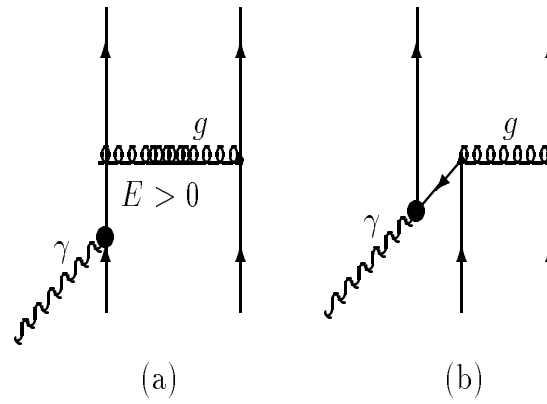


Figure 4:

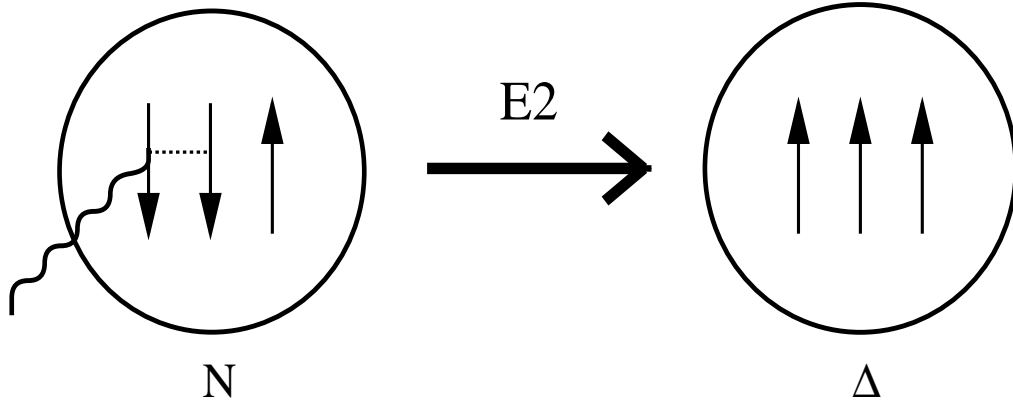


Figure 5:

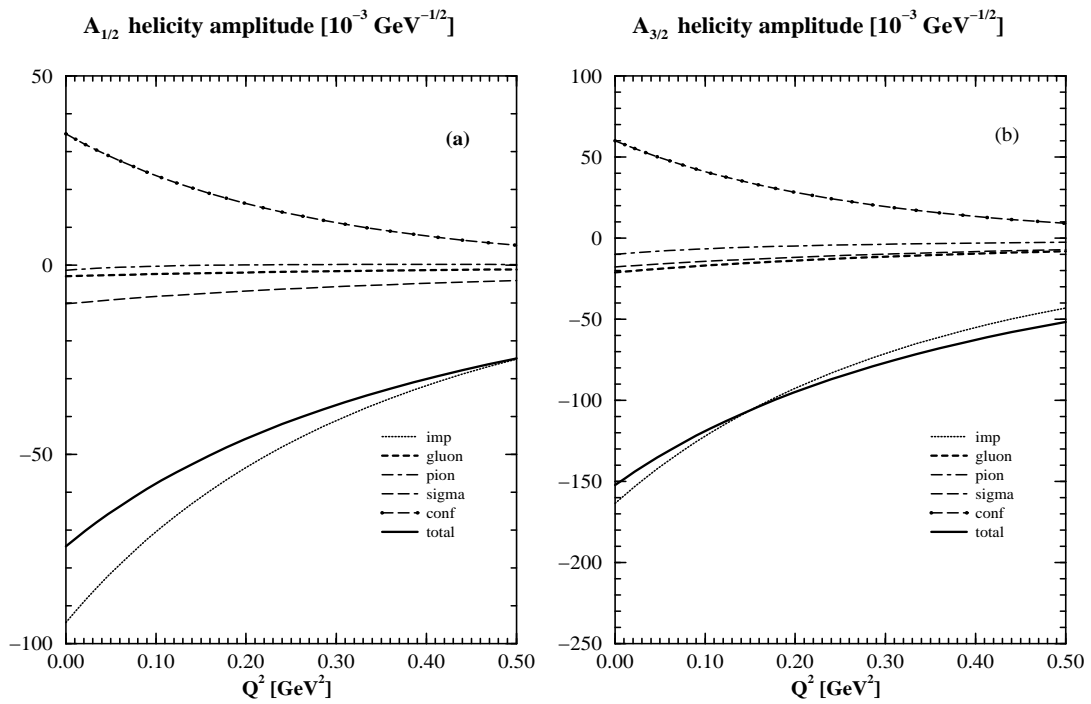


Figure 6: